DTIC
S ELECTE
JAN 07 1991
B D

LOW TEMPERATURE PHOTOLUMINESCENCE
STUDY OF HOLMIUM AND THULIUM IMPLANTE
INTO III-V SEMICONDUCTORS AND SILICO

THESIS

Eric Silkowski, B.A.
First Lieutenant, USAF

AFIT/GEP/ENP/90D-7

DEPARTMENT OF THE AIR FORCE

AIR UNIVERSITY

AIR FORCE INSTITUTE OF TECHNOLOGY

LOW TEMPERATURE PHOTOLUMINESCENCE
STUDY OF HOLMIUM AND THULIUM IMPLANTED
INTO III-V SEMICONDUCTORS AND SILICON

THESIS

Eric Silkowski, B.A.
First Lieutenant, USAF

AFIT/GEP/ENP/90D-7

DTIC
S ELECTE
JAN 0 7 1991
B
D

Approved for public release; distribution unlimited

AFIT/GEP/ENP/90D-7

LOW TEMPERATURE PHOTOLUMINESCENCE STUDY OF

HOLMIUM AND THULIUM IMPLANTED INTO

IlI-V SEMICONDUCTORS AND SILICON

THESIS

Presented to the Faculty of the School of Engineering

of the Air Force Institute of Technology

Air University

in Partial Fulfillment of the

Requirements for the Degree of

Master of Science in Engineering Physics

Eric Silkowski, B.A.

First Lieutenant, USAF

December, 1990

Acknowledgements

I wish to thank my thesis advisor, Professor Y. K. Yeo, for his continued encouragement and guidance in my studies of solid state physics. I wish to specially thank Capt. José E. Colön for his many hours of patience and tutoring in the laboratory. Many of the samples used in this study were graciously provided by Maj. Gernot S. Pomrenke of the Air Force Office of Scientific Research. Thanks also go to Ian Brown of the University of California for implantion of samples used in this study. Also, the Avionics Laboratory was kind enough to allow me the use of their annealing facilities. I must also not forget to thank Mr. Greg Smith for all of his work in keeping the laboratory running smoothly.

I must express my deepest gratitude to my wife, M. Christina Dobrowolski, for her understanding, patience and support during this entire eighteen month period, not to mention her proof-reading, editing, and objective viewpoint. Finally, I want to thank my son, Alexander Tomasz Silkowski Dobrowolski, for being there to brighten my days.

Eric Silkowski

Accession For	
NTIS GRA&I	☑
DTIC TAB	☐
Unannounced	☐
Justification	

By	
Distribution/	
Availability Codes	
Dist	Avail and/or Special
A-1	

ii

Table of Contents

List of Figures

List of Tables

Abstract

Low temperature photoluminescence studies were performed on holmium and thulium implanted III-V semiconductors and silicon. Specifically, holmium was implanted into InP, GaAs, and Si; and Tm in AlGaAs, GaAs, and Si. To repair lattice damage caused by implantation and activate the 4f emissions, these samples were annealed at various temperatures by the conventional furnace and rapid thermal techniques.

None of the characteristic 4f emissions of holmium were found in any of the implanted samples in the spectral region of .73 to 1.55 eV (.8 to 1.7 μm).

AlGaAs:Tm showed strong thulium 4f emissions in the .93 to 1.03 eV (1.2 to 1.35 μm) region. These emissions were studied and compared to those in GaAs:Tm. Low and high temperature annealed samples showed evidence of different Tm^{3+} centers. Temperature dependence studies showed that thulium 4f emissions were present above 200 K, but quench by about 240 K. Laser excitation power dependence studies showed that the luminescent intensity of the main thulium 4f line depends linearly on the square root of excitation laser power. This result implies that non-radiative decay mechanisms compete with the excitation and subsequent radiative decay of the thulium 4f shell.

Also observed for the first time were thulium 4f emissions in the .93 to 1.03 eV (1.2 to 1.35 µm) region in high purity silicon implanted with thulium. Thulium 4f emissions were not observed in n and p doped silicon.

LOW TEMPERATURE PHOTOLUMINESCENCE STUDY OF

HOLMIUM AND THULIUM IMPLANTED INTO

III-V SEMICONDUCTORS AND SILICON

I. Introduction

The rare earth elements (RE), those numbered fifty-eight through seventy-one in the lower end of the periodic table, have properties which make them of interest for optical devices. When RE ions are incorporated into a host material, the electrons in their 4f shells are screened from outside forces and therefore their energy levels should be insensitive to host material and temperature. Hence, 4f-4f radiative transitions would be sharp, frequency stable spectral lines, a situation unlike that of conventional semiconductor diodes and lasers. [For example, a GaAs diode emits at 1.37 eV at 295 K but 1.48 eV at 77 K (Sze, 1981:686).] Therefore, RE ions in III-V compounds and silicon are of interest since they may be potential candidates for compact, electronically excited light emitting or laser diodes.

REs have already proven their usefulness in traditional laser applications in such ionic materials as LaF_3 and CaF_2 (DiBartolo, 1968:521-523). In fact, a very common laboratory tool is the Nd:YAG laser which utilizes 4f-4f

1

emissions. Ionic materials, however, only allow the possibility of optical pumping due to their insulating behavior. Semiconductor materials, on the other hand, allow the possibility of excitation by electrical means.

Since REs have only recently been studied in III-V compounds and silicon, there is much to be learned. For example, the excitation mechanisms of 4f luminescence are very poorly understood. If one could understand the excitation process fully, it might allow the fabrication of new electro-optic devices. Also, not all REs have been examined for radiative emission in the most common III-V compounds such as GaAs, InP, GaP, and AlGaAs.

The first step in determining whether REs will be useful in the electro-optics area is to determine if and under what conditions radiative 4f-4f transitions occur. For this purpose, photoluminescence will be used.

Photoluminescence will determine whether the characteristic 4f-4f emissions are present in a particular sample. This technique is also non-destructive allowing the sample to be used in further experimentation. Furthermore, once the emissions are seen and the wavelength determined, time-resolved photoluminescence and excitation spectroscopy can be performed to better elucidate the mechanics of the excitation.

Photoluminescence does have some limitations; however, the main limitation being that only radiative transitions

can be observed. Only by observing the quenching of a photoluminescence feature can a non-radiative process be inferred. Also, no direct information on energy levels can be obtained; only transition energies between two levels can be observed. Furthermore, in semiconductors, this energy difference must be smaller than the bandgap or the energy will be reabsorbed by the crystal.

This study had two main thrusts. First, holmium implanted Si, InP, and GaAs were examined to determine if 4f emissions were present. These samples were annealed under various conditions to determine whether optically active holmium centers were formed and what optimal annealing conditions might be.

Second, thulium emissions in the .93 to 1.03 eV (1.20 to 1.35 μm) region were examined in AlGaAs and GaAs. This is the first observation of optically active thulium centers in AlGaAs. Since only four AlGaAs:Tm samples, three of the same Al concentration, were available, only limited anneal temperature comparisons would be possible. No meaningful Al concentration study could be performed with this limited sample set. Since a previous temperature quenching study was done on the GaAs:Tm samples, a similar experiment was performed on AlGaAs:Tm for comparison purposes. Neither GaAs:Tm nor AlGaAs:Tm emissions had been previously studied as a function of excitation power. Since such a study can help in understanding excitation mechanisms it was performed

3

in this work. Finally, a small sample set of silicon

implanted with thulium were examined in the .93 to 1.03 eV

(1.20 to 1.35 μm) region to ascertain whether 4f emissions

were present.

II. Background and Theory

Semiconductors

Semiconductors are a class of materials that are insulators at temperatures near zero Kelvin, but have observable conductivity at room temperature (Ashcroft and Mermin, 1976:562). This strange behavior is well explained by the theory of band structure.

When atoms are assembled in a solid, their electronic wavefunctions overlap. This overlap causes the discrete energies of the allowed levels of the atom to become 'smeared' into a wide range of energies. These allowed ranges of electron energy are called bands, and a given number of electrons are allowed to fill each. Energy regions which are not allowed are called 'forbidden bands'. Since electrons are fermions with half-integral spin, two cannot occupy the same quantum state of a given band. One can then think of bands as 'filling' with electrons from the lowest energy to the highest energy.

According to band theory, any completely filled band cannot conduct; only partially filled bands can conduct (Ashcroft and Mermin, 1976:221-223). Metals, which conduct very well, have a partially filled uppermost band, as shown in Figure 1. Insulators, on the other hand, have a completely filled uppermost band. The next band above is
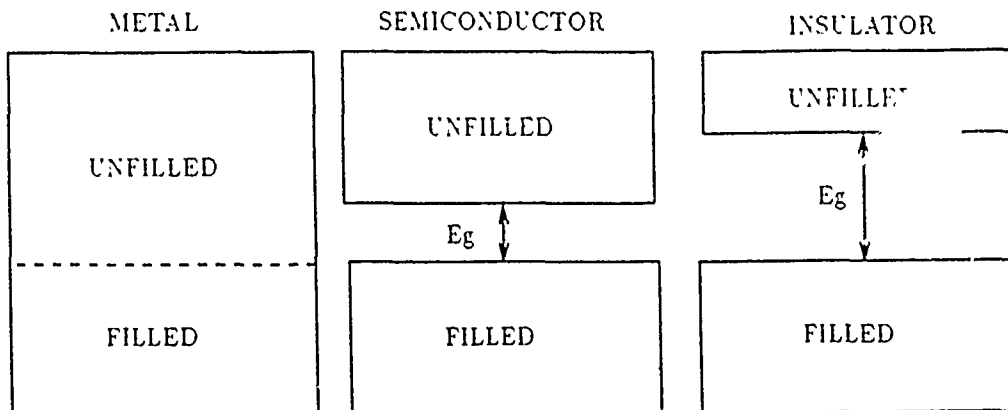
Figure 1. Band Structure of Metals, Insulators, and Semiconductors

separated in energy by a gap, E_g, which is usually more than 5 eV from the top of filled band, and so very high energy would be needed to promote an electron from the filled band to the unfilled band. Therefore, for insulators, the thermal energy available at room temperature or that obtained with typical applied electric fields is not enough to cause a significant number of electrons to be promoted to the upper band. Semiconductors have a band gap which is just small enough that at room temperature enough electrons can gain energy in excess of the band gap to give a measurable conductivity. Table 1 lists band gaps and several other properties of semiconductors of interest to this study.

When an electron 'jumps' from the filled or valence band to the unfilled or conduction band, it leaves behind a vacancy in the valence band. This lack of an electron is called a hole. Band theory shows that a hole acts like a positively charged electron (Ashcroft and Mermin, 1976:225-

6

229). Holes can participate in conduction just as electrons do.

Electrons and holes have been found to interact with one another. One such interaction is called an exciton. Excitons have been defined as a type of electronic excitation which is able to transport energy but not charge (Kabler, 1988:296). In the Mott-Wannier model (Kabler, 1988:296), excitons are thought of as an electron in the conduction band weakly bound to a hole in the valence band by Coulomb forces. Excitons are not localized at any one particular atom, and, in fact, they overlap many atoms in

TABLE 1
Selected Semiconductor Properties

		InP	GaP	GaAs		Si
Bandgap (eV)						
0 K	:	1.42	2.34	1.52		1.17
300 K	:	1.35	2.26	1.42		1.12
Crystal Structure	:	ZB	ZB	ZB		Dia
m_e^*/m_e	:	.077	.82	.067	L	.98
					T	.19
m_h^*/m_e	:	.64	.60	.082	l	.16
					h	.49
k	:	12.4	11.1	13.1		11.9

Dia = Diamond structure   ZB = Zincblende structure
L = longitudinal effective mass l = light hole
T = transverse effective mass   h = heavy hole
k = static relative dielectric constant
(after Sze, 1981:849)

the crystal. The binding energy of an exciton is given
by:

$$E_{ex} = -m^* e^4 / 2h^2 k^2 n^2 \qquad (1)$$

where m^* is the reduced mass formed from the conduction
band effective mass, m_c^*, and the valence band effective
mass, m_v^*; e is the electron charge; h is Planck's constant
divided by 2π; k is the static dielectric constant; and
finally n, which must be a positive integer, is a quantum
number indicating the excitonic state (Pankove, 1971:12).
Exciton energy levels are not well defined within the
bandgap, but are typically defined with relation to the
bottom of the conduction band. The n=1 exciton is farthest
from the conduction band edge while increasing values of n
are closer until the n equals infinity level is at the
conduction band. (See Figure 2.)
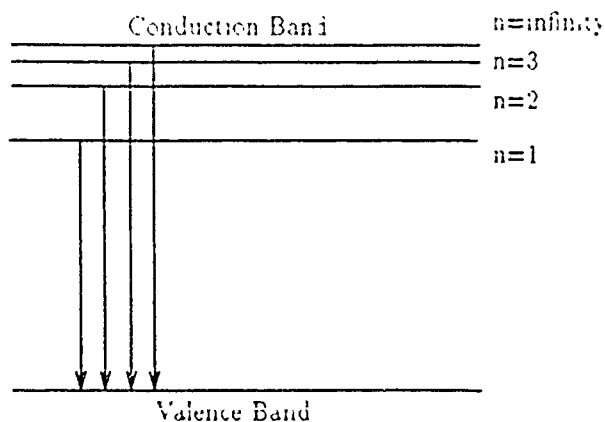
Figure 2. Exciton Energy Levels

Until now only pure, perfectly crystalline semiconductors have been considered. But even state of the art production methods leave impurities in semiconductor crystals. These impurities often lead to energy levels which fall within the band gap. Those levels which fall just below the bottom of the conduction band are called donor levels. For instance, when an element from the sixth row of the periodic table is found in a III-V compound, it usually substitutes on the anion site. Since it has one more electron than the anion it replaces, this electron needs only a small amount of energy, E_d, to liberate it from its localized level about the atom and move it into the conduction band. An example of this type of donor is sulfur in GaAs which substitutes on the As site (Sze, 1981:21). Similarly, an element of the second row of the periodic table will substitute for the cation in a III-V compound. This impurity has one less electron than a cation from the third group of the periodic table and so if an electron in the valence band gives up a small amount of energy, E_a, it can form a localized level about this impurity. This type of impurity is called an acceptor since it can take an electron from the valence band leaving a hole behind. An example of this type of acceptor is beryllium in GaAs (Sze, 1981:21). Donors and acceptors, having one too many or one too few electrons, respectively, behave very much like hydrogenic atoms. The ionization, or

9

behave very much like hydrogenic atoms. The ionization, or binding energy, of the electron or hole is given by:

$$E_{d,a} = m^* e^4 / 2h^2 k^2 n^2 \qquad (2)$$

where m* is the reduced mass formed from the nuclear mass and the electron or hole effective mass, and the other variables are as described for equation 1 (Pankove, 1971:9).

Substitutional impurities are not the only way to produce donors or acceptors. An example is a missing atom, also called a vacancy, which can sometimes produce an acceptor or donor.

When there are significant amounts of impurities present in a semiconductor, they can significantly alter the material's conductivity. In the situation of donors, the semiconductor has many corduction electrons but very few holes. Since the charge carriers are negative, the conductivity is called n-type. In the opposite situation, an abundance of acceptors leads to an abundance of holes and hence positive conductors or p-type.

Another type of impurity does not change electrical properties and is called the isoelectronic trap. When an impurity atom substitutes for a host atom with the same valence, a localized potential is created. If this potential captures an electron, then the trap becomes

10

charged. Once charged the trap will attract holes, hence bound excitons can be formed (Pankove, 1971:61).

All of the semiconductors involved in this study have tetrahedral coordination. In other words, each lattice site has four nearest neighbors arranged at the vertices of a tetrahedron. The tetrahedral structure can be described as two interpenetrating face centered cubic (fcc) lattices. One sublattice starts at position (0,0,0) and the second sublattice begins at (1/4,1/4,1/4). (See Figure 3.) In an elemental material like silicon, both sublattices are filled with silicon atoms. This arrangement is called the diamond structure. In a binary compound such as GaAs, gallium atoms fill one sublattice while arsenic fills the other. This arrangement is called the zincblende structure. Ternary compounds such as AlGaAs, have one sublattice shared by Al and Ga while the other remains exclusively As.

(a)   (b)
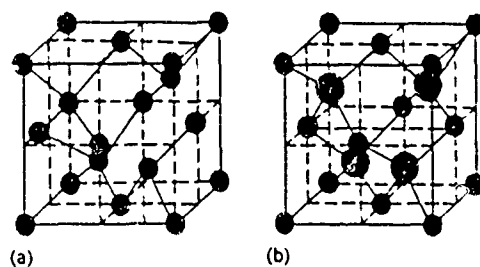
Figure 3. Diamond (a) and Zincblende (b) Structures (Dekeyser, 1988:15)

It is known that in any close packing of spheres, of which a fcc lattice is one example, that there is one

11

octahedral and two tetrahedral voids per lattice site
(Mooser, 1986:26). A tetrahedral structure can be thought
of as a fcc structure with one half of the tetrahedral
voids filled by the second sublattice. This scheme leaves
one octahedral and one tetrahedral void per lattice site.
Together the tetrahedral space about each atom, the one
tetrahedral void, and the one octahedral void fill space
(Mooser, 1986:26-27). (See Figure 4.)
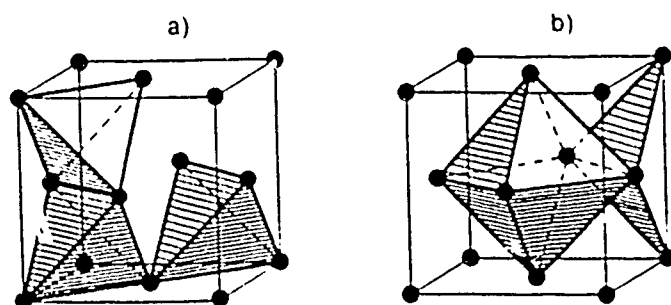
Figure 4. Tetrahedral (a) and Octahedral voids in a
Tetrahedral Lattice

Any impurity atoms which enter the lattice must then
substitute for an atom of the lattice or fill one of the
voids. An impurity, especially a large ion, is unlikely to
be found in between bonds. If an ion were in between
bonds, its electronic shells would overlap with the bonds,
producing an energetically unfavorable situation due to
Coulomb repulsion. So it can be concluded that impurities
will be found predominately at sites of octahedral or
tetrahedral symmetry in tetrahedrally coordinated
compounds. One note of caution, however, is that large

12

ions can distort the surrounding lattice lowering the symmetry of the site. This type of behavior would also lead to inhomogeneous line broadening.

Photoluminescence

When electromagnetic waves of energy greater than the bandgap impinge on a semiconductor, that radiation will be absorbed, and electrons from the valence band will be promoted to the conduction band. These excited electrons are then able to give up their energy in a number of ways. One of the most easily detected energy loss mechanisms is a radiative transition; light of energy below the bandgap is emitted. This process of light absorption and re-emission is called photoluminescence.

The first question in the interpretation of photoluminescence spectra is 'what transitions can one expect to observe?'. For most semiconductors, there are several processes which give rise to detectable peaks. Some of the most common are band to band, donor-acceptor pair recombination, acceptor free-to-bound, donor free-to-bound, and both free-excitons and excitons bound to impurities. (See Figure 5.) Strong phonon coupling often prevents levels which lie deep within the band gap from decaying radiatively, hence most emissions are seen near the band edge and are called "near edge emissions" (Dean, 1982:10).

13

CONDUCTION BAND
EXCITON LEVEL
DONOR LEVEL
ACCEPTOR LEVEL
VALANCE BAND
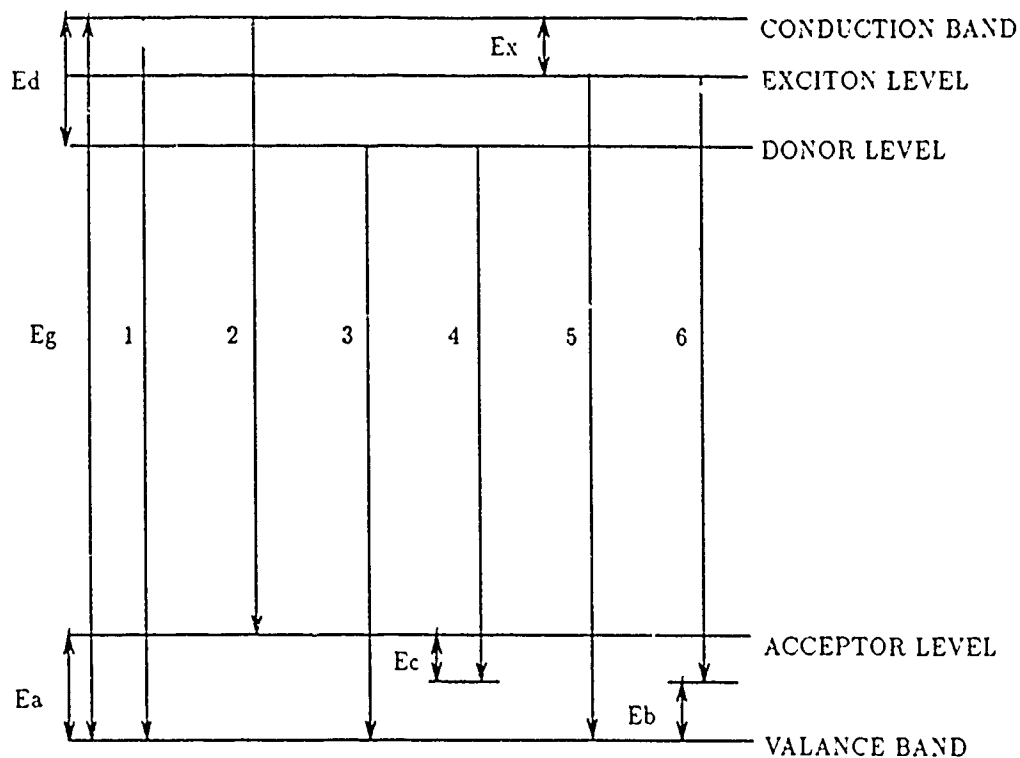
1: BAND TO BAND
2 ACCEPTOR FREE-TO-BOUND
3 DONOR FREE-TO-BOUND
4 DONOR-ACCEPTOR PAIR
5 FREE EXCITON
6 BOUND EXCITON

Eg=Energy Gap
Ed=Donor Energy
Ea=Acceptor Energy
Ex=Exciton Energy
Ec=DA Coulomb Binding Energy
Eb=Exciton Binding Energy

Figure 5. Radiative Transitions in Semiconductors

Band to band emissions are simply due to the recombination of an electron in the conduction band with a hole in the valence band. Consequently, the minimum energy photon emitted has the energy of the band gap. However, unless the sample is optically thin, most above gap emission will be reabsorbed before it exits the semiconductor. In PL spectra, therefore, only significant

14

emissions are seen below the band gap. Band to band
transitions are a major source of absorption and PL relies
on this fact.

Donor acceptor (DA) pair transitions are another
possibility. An electron at a donor can combine with a
hole at an acceptor. There is a Coulomb attraction between
the electron and hole involved and this adds an energy
term, $E_c = e^2/kr$. The transition energy is given by:

$$E = E_g - E_d - E_a + e^2/kr + E_p \qquad (3)$$

where r is the distance between donor and acceptor pair, e
is the electron charge, k is the static dielectric
constant, and E_p is the polarization interaction term
(Dean982:119). Since the atoms in a crystal are at fixed
lattice sites, the allowed values of r are restricted.
Therefore, a number of sharp lines can be seen in the DA
spectra of some semiconductors. However, the sharp line
spectra begin to overlap for r larger than 4 nm forming a
broad band (Pankove, 1971:143).

Free to bound transitions come in two varieties.
First, an electron in the conduction band can recombine
with a neutral acceptor. The energy of this transition is
given by:

$$E = E_g - E_a \qquad (4)$$

Second, a hole in the valence band can recombine with a neutral donor. The energy of this transition is given by:

$$E = E_g - E_d \qquad (5)$$

Another major cause of near-edge emissions are excitons. Since their binding forces are weak, free exciton spectra are only observable in sufficiently pure samples at low temperatures (Pankove, 1971:114,124). E_{ex} is also typically smaller than E_d or E_a. This relation is explained by noting that m_c^* and m_v^* are about the same order of magnitude and both are less than $m_{electron}$; whereas, for the donor or acceptor level the reduced mass is approximately equal to the electron mass. Since both donor and exciton are described by the same energy level equation (equations 1 and 2), this disparity in reduced mass becomes a difference in energy.

Excitons are unstable against decay recombining radiatively or nonradiatively. The transition energy is given by:

$$E = E_g - E_{ex} - E_{phonons} \qquad (6)$$

where $E_{phonons}$ is energy carried off by any phonons that may be emitted in the process. The lifetime of a free exciton is often long enough to allow trapping on an impurity, with the formation of a bound exciton (Kabler, 1988:298). When binding occurs, the resulting emission is

16

1988:293). When binding occurs, the resulting emission is also characteristic of the impurity.

Excitons can become bound to donors, acceptors, or isoelectronic traps. Each such impurity has a characteristic binding energy, E_b, which is required to liberate the exciton from the impurity. The transition energy for a bound exciton is given by:

$$E = E_g - E_{ex} - E_b \qquad (7)$$

Another source of lines in the photoluminescence spectra is due to phonon replicas. Interaction of the dynamic modes of the crystal lattice with optical radiation can occur resulting in the emission of or absorption of one or several phonons. Since there are very few phonons available for absorption at low temperature, phonon replicas appear in low temperature spectra only on the low energy side of the zero phonon line.

Rare Earth Ions

Rare Earth elements as a group show very similar chemical behavior since they possess similar outer electronic structure, namely filled 5s, 5p and 6s shells. The Rare Earths differ only in their filling of the 4f shell. When a Rare Earth ion is within a crystalline lattice, however, it is often in the trivalent state, Re^{3+}. The 4f electrons are screened from any fields external to

17

the ion by the outer filled 5s and 5p shells. Therefore, any radiative transitions within the 4f shell should occur at nearly the same frequency as those for the free ion. This screening implies that transition frequencies are nearly independent of the host crystal and of temperature. Also, the transitions should be the same regardless of the lattice site of the Rare Earth, that is, whether the ion is substitutional or interstitial and what its nearest neighbors are. Consequently, any electro-optic devices utilizing such a 4f-4f transition would have linewidths only limited by the homogeneous linewidth of the transition.

'How are the energy levels of the RE's described?'. First, we must understand the electronic configuration of a RE ion incorporated in a solid. The RE's are often in the trivalent state within the material and therefore have the configuration shown in Table 2. As is easily seen from the table, the 4f shell fills with from one to fourteen electrons as one progresses in atomic number. All RE^{3+} have a Xe 'core' in common, namely:
$1s^2 2s^2 2p^6 3s^2 3p^6 3d^{10} 4s^2 4p^6 4d^{10} 5s^2 5p^6$.

To understand the available energy levels of such an electronic configuration, one must understand the Hamiltonian which describes this n electron system. If the RE ion is found in a crystalline environment which only

18

TABLE 2
Electronic Configuration Of RE^{3+}

Atomic Number	Symbol	Electronic Configuration	Term
58	Ce	$4f$	$^2F_{5/2}$
59	Pr	$4f^2$	$^3H_4$
60	Nd	$4f^3$	$^4I_{9/2}$
61	Pm	$4f^4$	$^5I_4$
62	Sm	$4f^5$	$^6H_{5/2}$
63	Eu	$4f^6$	$^7F_0$
64	Gd	$4f^7$	$^8S_{7/2}$
65	Tb	$4f^8$	$^7F_6$
66	Dy	$4f^9$	$^6H_{15/2}$
67	Ho	$4f^{10}$	$^5I_8$
68	Er	$4f^{11}$	$^4I_{15/2}$
69	Tm	$4f^{12}$	$^3H_6$
70	Yb	$4f^{13}$	$^2F_{7/2}$
71	Lu	$4f^{14}$	$^1S_0$

(after Pappalardo, 1978:176)

exerts a weak electric field on the ion, then one can use
the following approach (DiBartolo, 1968: 196-197). The
Hamiltonian used is the free ion Hamiltonian with an
additional small perturbation due to the crystal field.
Thus the Hamiltonian is:

$$H = H_0 + H_{ee} + H_{so} + H_{cf} \qquad (8)$$

where H_0 is the contribution from each electron's motion
about the nucleus, H_{ee} is the electron-electron interaction
term, H_{so} is the spin-orbit interaction term, and finally
H_{cf} is the crystal field contribution. These terms are
further described in the appendix.

If one first neglects the H_{cf} term and concentrates on
the free ion Hamiltonian, one can solve the Schrodinger

equation to obtain the spin-orbit energy levels. These energy levels and their allowed transitions will be insensitive to temperature and crystalline environment as discussed above. The usual symbol, $^{2s+1}L_J$, is used to label these 'terms'. It should be emphasized that use of this term symbol implies that S, the total electronic spin, L, the total orbital angular momentum, and J, the total angular momentum are observables for the system. Spin-orbit levels for the RE^{3+} ions have been determined and are shown in Figure 6.

When the crystal field term of the Hamiltonian is taken into account, it breaks the full rotational symmetry implied by the above spin-orbit terms. If the ion is found in a local environment which has octahedral symmetry for example, then the spin-orbit terms can be split into several energy levels reflecting this octahedral symmetry.

Selection Rules

Electric dipole transitions are normally the strongest radiative transitions possible; therefore, knowing which transitions are electric dipole allowed greatly aids in the interpretation of spectra. The electric dipole operator for ions in crystalline fields is much more complicated than for free ions. In fact, selection rules are influenced by the site symmetry of the emitting RE ion.
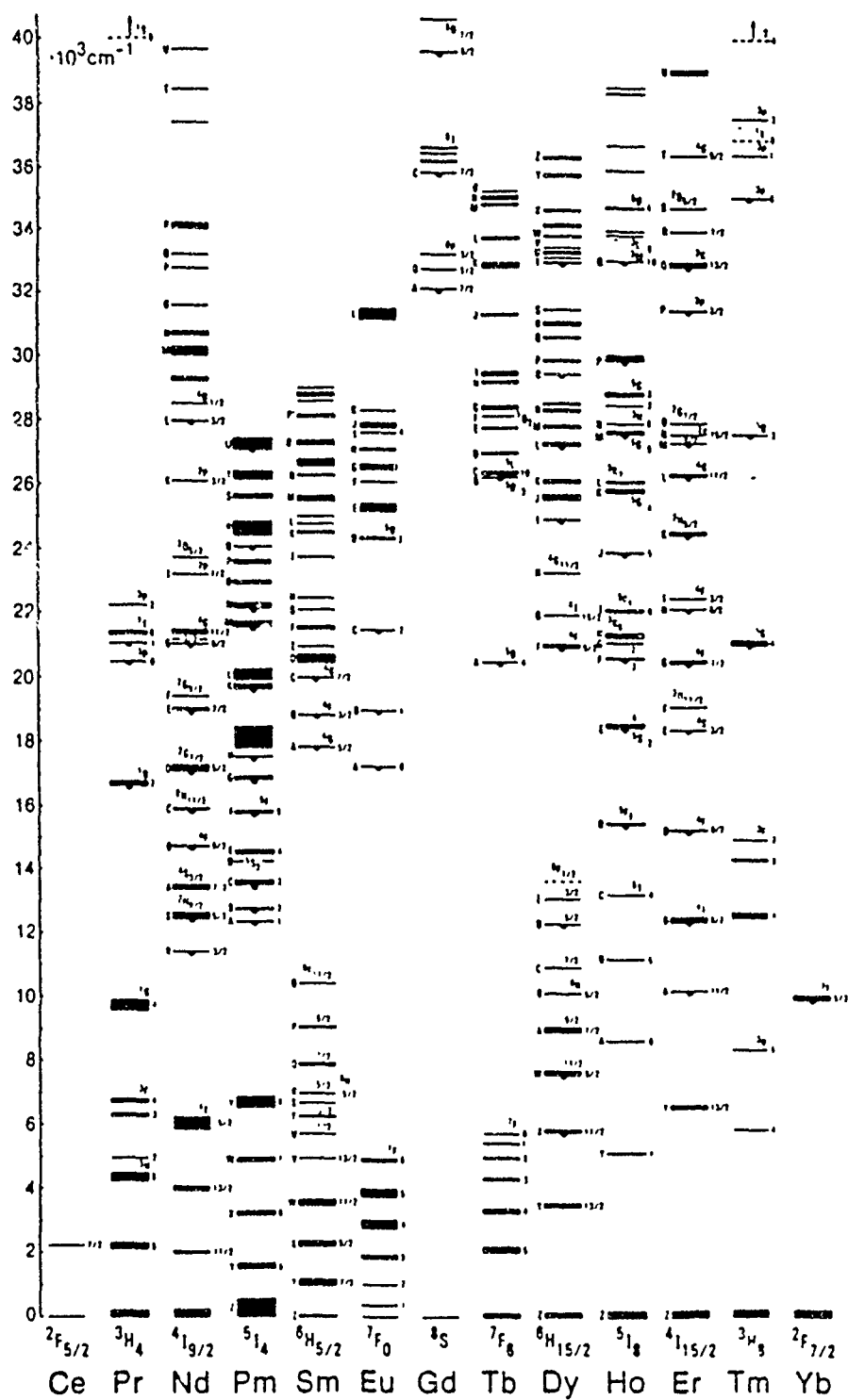
Figure 6. Energy Level Diagram for RE^{3+} in LaCl$_3$.
(Imbusch and Kopelman, 1986:8)

For the RE ions, the crystal field has only a weak effect on the 4f levels, and therefore the free ion selection rules still have some validity (DiBartolo, 1968:332-333). Since for the free ion electric dipole transitions are disallowed between 4f levels, it is only the small crystal field perturbation that makes electric dipole transitions possible. Selection rules are therefore totally dependent on RE ion site symmetry.

Electric dipole selection rules do exist for 4f-4f transitions. Judd (1962) and Ofelt (1962) used the fact that the crystalline field can cause configuration interaction of the $(4f)^n$ and $(4f)^{n-1}5d$ configurations to derive some general selection rules for 4f-4f electric dipole transitions. These selection rules are:

a. $|J'-J| < 6$
b. for RE ion with even number of electrons
    i. $J=0$ to $J'=0$ is forbidden
    ii. $J=0$ to odd J' are weak
   iii. $J=0$ to $J'=2,4,6$ should be strong
    iv. $J=1$ to $J'=2$ should appear only in σ polarization

(Imbusch and Kopelman, 1981:9).

It should also be noted that crystal field effects can lead to mixing of J levels and cause relaxation of these selection rules (Imbusch and Kopelman, 1981:9).

For the special case of cubic symmetry, including tetrahedral and octahedral coordination, no polarization effects are present; therefore, any RE radiation would be isotropic (DiBartolo, 1968:335).

Previous Work On RE Doped III-V Compounds And Silicon

Past studies of RE in III-V compounds have mainly concentrated on ytterbium in InP and erbium in GaAs. It is these two elements which are therefore most understood. Pomrenke (1989:21-32) reviews much of the past work on these materials. Luminescence has also been observed for Nd in GaP and GaAs, Pr in GaP, Sm in GaP, Dy in GaP, and Ce in GaP. The only work on thulium aside from Ennen and Schneider's (1984:124) brief mention of 1.2 µm emissions is that of Pomrenke (1989) at AFIT. 4f emissions have not been reported for Pm, Eu, Gd, Tb, Ho, or Lu.

Much of the recent work on RE doped III-V materials has concentrated on excitation mechanisms of the 4f levels. Various mechanisms have been proposed. These include excitation by free charge carriers, donor-acceptor pair Auger recombination, and capture of excitons.

Early studies (Kasatkin and Savel'ev, 1984; Kasatkin et al., 1985) suggested that donor-acceptor pair recombination and subsequent non-radiative energy transfer to the RE was responsible for 4f excitation. Korber and Hangleiter (1988:116) concluded from photoluminescence excitation spectroscopy that free charge carriers are necessary for excitation of Yb in InP, but that actual excitation may occur by exciton capture. They ruled out the possibility of donor-acceptor transfer. Takahei et al.

(1989) believe that Yb acts as an acceptor-like electron trap near the conduction band edge. 4f excitation would then take place when an electron trapped at the Yb level combines with a hole at an acceptor or in the valence band. Recently, Benyattou et al. (1990) proposed a model in which bound excitons were the excitation source for Er in AlGaAs.

III. Experimental Procedure

Sample Preparation

The samples used in this study were all previously implanted with RE ions. The implantations were performed using ion accelerators with energies of either 100 keV, 390 keV, or 1000 keV. The dosage used was 3×10^{13} ions/cm^2 for holmium and 5×10^{13} ions/cm^2 for thulium. The implantation process causes crystal damage due to the impact of the large, energetic RE ions.

To repair the lattice damage and 'activate' the RE's luminescence, most samples were annealed by the conventional furnace method. (See Figure 7.) A glass tube was placed inside the furnace heating chamber, and samples were slid into this tube on a glass 'boat'. The furnace was regulated by a Eurotherm temperature controller which used a thermocouple inside the sample tube. Inert gas flowed over the sample during annealing to prevent oxidation. This gas was either nitrogen or forming gas, a mixture of 4.84 percent hydrogen and 95.16 percent argon.

The samples were also protected from dissociation of host atoms and contaminants during annealing by use of the proximity method. A substrate of the same material was set face up on the sample boat and then the implanted sample was put face down upon it. Therefore, the sample's face
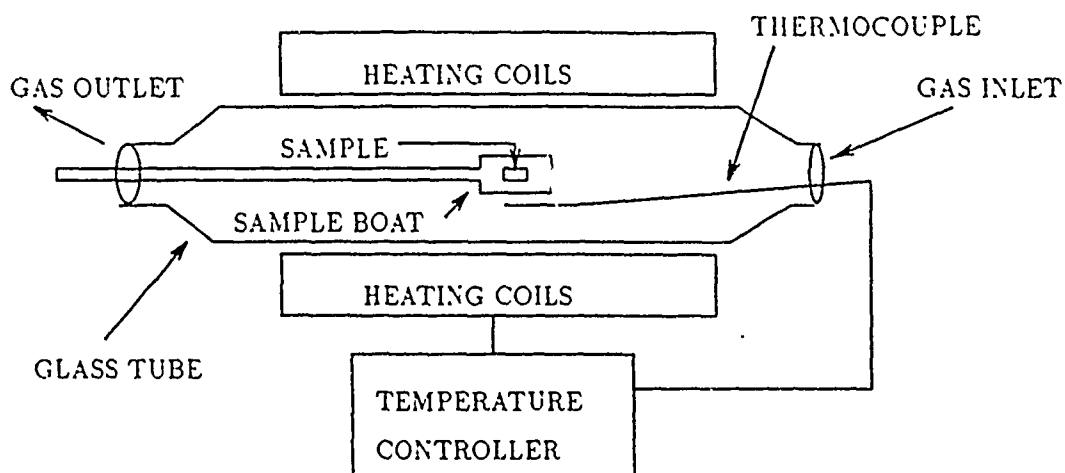
Figure 7. Conventional Annealing Setup

remained in contact with only material of the same chemical composition, and contamination was kept to a minimum.

A small number of samples were previously annealed by the rapid thermal annealing method (RTA). This method was described by Pomrenke (1989).

At various stages in the above preparation process, the samples required cleaning. They were individually cleaned to remove any surface contaminants such as grease or dust. The cleaning process consisted of spraying with liquid trichloroethylene, followed by acetone, followed by methanol, and finally de-ionized water. The sample was then blown dry using dry nitrogen gas.

Photoluminescence Measurements

Photoluminescence was performed using the experimental setup shown in Figure 8. The samples were cooled in a

26

Figure 8. Laboratory Setup for Photoluminescence Experiments.

27

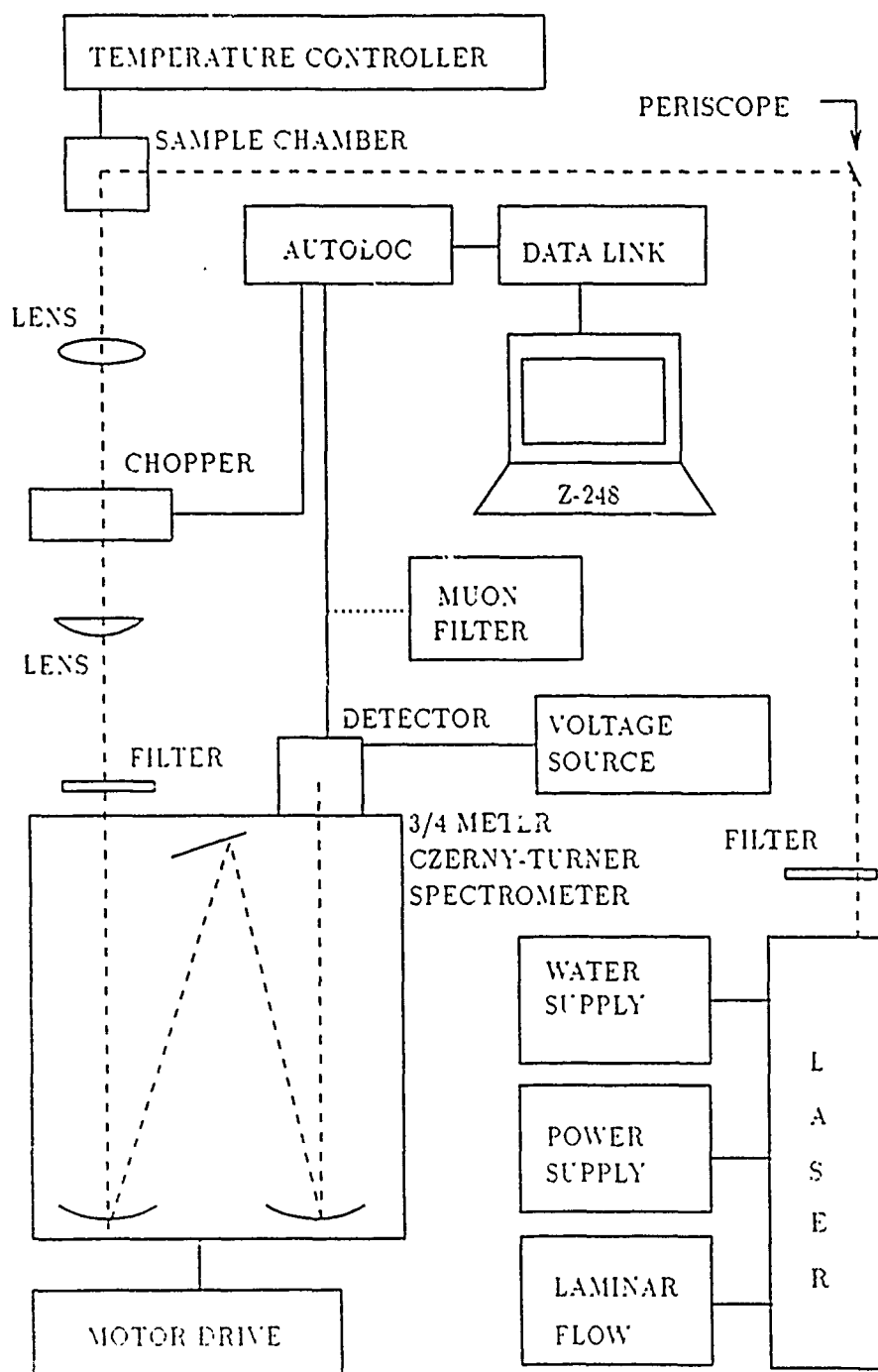Janis Research model 10DT dewar. They were mounted with rubber cement onto a stainless steel mounting block. This block was lowered into the bottom of the dewar where it could be cooled.

Before cooling, the dewar walls were pumped to vacuum with a Duo-Seal model 1397 mechanical vacuum pump followed by a Leybold-Heraeus Turbovac TMP-360 turbomolecular pump. The vacuum gauge system could be degassed with a Veeco Instruments model RG-83 ionization gauge control unit. The vacuum pumping was performed exclusively on the cryogenic casing of the dewar; the sample chamber itself was never pumped to vacuum. Before cooling, however, the sample chamber was flushed with 2 psi helium gas in order to remove water vapor. If ice were to form within the chamber it could potentially block the flow of liquid helium.

Next, liquid nitrogen followed by liquid helium were added to the dewar resevoir. A Lake Shore Cryogenics model DRC 82C temperature controller unit was used to control the sample temperature. Also, the flow of liquid helium through the needle valve to the sample chamber allowed adjustment of the sample temperature from 4.2 K to room temperature. To attain 4.2 K, the sample itself was immersed in liquid helium. This immersion caused some attenuation of the laser beam and additional noise in the output signal due to the boiling action of the LHe. Many spectra were therefore taken at 6 K to alleviate the above problem.

The excitation source used was a Spectra-Physics model 2020-11 Krypton Ion laser with a model 2560 power supply, model 314 ion laser water conditioning system and a model 2200 laminar flow unit. This source produced 647.1 nm wavelength light with a power range of up to 820 mW. Beam power measurements were done with a Coherent 210 power meter placed to intercept the entire beam.

To insure that only the 647.1 nm laser line reached the sample, a 650 nm band pass filter was placed prior to the sample in the beam path. The beam then reflected off a two mirror periscope and into the sample chamber. The emissions off the sample were collected with a spherical lens and passed through a chopper. Finally, the beam was focused unto the spectrometer slit with a cylindrical lens.

The spectrometer used was a SPEX model 1702 3/4 meter Czerny-Turner. It could be scanned at 5000, 1000, 250, 100, 50, 25, 5, 1, and .5 Å/min and typical speeds used were from 250 to 5 Å/min. The grating used was blazed at 1.6 μm. Most scans were performed in second order. The use of second order allowed for a factor of two increase in resolution. Also, using second order allowed the slit width to be opened to double that of first order thereby allowing higher throughput. Since many of the signals being measured were weak, this increase in light throughput was essential. The exit slit of the spectrometer was always kept at twice the entrance slit width, as

always kept at twice the entrance slit width, as recommended by the manufacturer.

The spectrometer output signal was detected with two different setups in order to cover different frequency ranges. In the 600 nm to 1000 nm range, an RCA S-1 photomultiplier tube was used and in the 800 nm to 1700 nm range, a Ge photo-detector was used. The S-1 tube wa kept at liquid nitrogen temperature with a Products for Research LN2 cryostat controller. The S-1 was biased at -1800 V and its signal was amplified with a Keithley 427 current amplifier. A gain of 10^8 V/A, suppression of 10^{-7} A, and a rise time of .03 ms were found to be appropriate settings.

The signal was then input into a Keithley 840 autoloc amplifier. An autoloc amplifier was used in order to screen out unwanted noise. The infrared region of the spectrum was very cluttered with stray radiation emanating from most objects at room temperature. Since it is impossible to shield the detector and the spectrometer from stray radiation, the autoloc must be used. The autoloc used phase sensitive detection to compare the signal (when the beam was allowed to pass) to the background (when the beam was blocked). The reference signal for the autoloc was provided by a 60 Hz four blade chopper which was in the beam path. Typical time constants used for the autoloc were 100 and 300 ms. The autoloc sensitivity was adjusted depending on the photoluminescent intensity, but typical

values used were 1 mV with a x10, x30, or x100 scale factor.

The Ge detector was also cooled with liquid nitrogen and was biased at -200 V. The Ge detector signal was then passed into the autoloc amplifier which was described earlier. A North Coast Scientific 829B muon filter was used to screen out signals generated by muons passing through the Ge. Typical settings used were gain of 50, hold of 130 ms, and integrate of .2 s.

The output from the autoloc was fed into a Zenith Z-248 computer via a data link. Since the data obtained in this way was in ASCII form, it was easily manipulated by such common software programs as Lotus 1-2-3.

In the production of the spectra shown in the results section, a factor of 1.23985 eV·µm was used to convert the wavelength output into the favored form, eV. It should also be noted that owing to the difficulty in obtaining absolute measures of intensity, the system response as a function of wavelength was not accounted for. All intensity readings are therefore reported in arbitrary units.

31

IV. <u>Results</u> <u>and</u> <u>Discussion</u>

<u>Holmium</u>

Holmium-implanted Si, GaAs, and InP were examined by
low temperature photoluminescence. If holmium was in the
trivalent state, then optical transitions to the spin-orbit
ground state $^5I_8$ were possible. Those most likely are the
three lowest energy transitions shown in Table 3. All of
these transitions are electric dipole allowed under the
Judd-Ofelt rules.

<u>TABLE 3</u>
Holmium Transition Energies

TRANSITION	ENERGY (eV)	WAVELENGTH (μm)
$^5I_5 - ^5I_8$	1.35 - 1.39	.89 - .92
$^5I_6 - ^5I_8$	1.04 - 1.08	1.15 - 1.19
$^5I_7 - ^5I_8$	.60 - .64	1.94 - 2.07

The transition energies shown in Table 3 are taken from the
energy level diagram shown in Figure 6. The range in
energies is due to the crystal field splitting of the spin-
orbit levels for the RE in an anhydrous trichloride crystal
(Imbusch and Kopelman, 1986:8-9). The splitting may be
different for the substrate materials examined here, but
the transitions will be in the same spectral region.
Pomrenke (1989) searched for emissions in the 2 μm region
and found none in these samples. This study therefore

32

concentrated on the 1.04 to 1.39 eV (.89 to 1.19 μm) range.

The sample set used is shown in Table 4.

<center>TABLE 4</center>
<center>Holmium Sample Set</center>

HOST	DOPANT	COND TYPE	IMPLANT ENERGY (keV)	ANNEAL TEMP/TIME/GAS	VENDOR*
InP	Fe	SI	100	none	MR
InP	Fe	SI	100	750°C/15 min	MR
InP	Fe	SI	1000	600°C/10 min	MR
InP	Fe	SI	1000	640°C/10 min/fg	MR
InP	Fe	SI	1000	650°C/15 sec/fg	MR
InP	Fe	SI	1000	700°C/15 sec/fg	MR
InP	Fe	SI	1000	750°C/15 sec/fg	MR
InP	Fe	SI	1000	800°C/15 sec/fg	MR
InP	Fe	SI	1000	850°C/15 sec/fg	MR
GaAs	?	SI	100	none	?
GaAs	?	SI	100	750°C/15 min	?
GaAs	?	SI	100	850°C/15 min	?
GaAs	?	SI	100	950°C/15 min	?
GaAs	und	SI	100	700°C/15 min/fg	MR
GaAs	und	SI	100	750°C/15 min/fg	MR
GaAs	und	SI	100	800°C/15 min/fg	MR
GaAs	und	SI	1000	750°C/15 min	?
GaAs	und	SI	1000	850°C/15 min	?
GaAs	und	SI	1000	950°C/15 min	?
Si	und	–	1000	650°C/15 min/N_2	W
Si	und	–	1000	750°C/15 min/N_2	W
Si	und	–	1000	850°C/15 min/N_2	W
Si	und	–	1000	950°C/15 min/N_2	W
Si	P	n	1000	750°C/15 min/N_2	PCA
Si	P	n	1000	850°C/15 min/N_2	PCA
Si	P	n	1000	950°C/15 min/N_2	PCA
Si	P	n	none	none	PCA
Si	P	n	none	750°C/15 min/fg	PCA

*MR is Metal Research, W is Wacker Siltronic, PCA is Polishing Corporation of America

InP:Ho

Eight annealed InP:Ho samples were examined in the .73 to 1.55 eV (.8 μm to 1.7 μm) spectral region which covers

<center>33</center>

the region of interest for the $^5I_5-^5I_8$ and $^5I_6-^5I_8$ Ho^{3+} transitions. Five of the samples were annealed by the rapid thermal annealing (RTA) technique, and the remaining three were conventionally annealed. All of the samples available were semi-insulating. No holmium-related peaks were found in any sample. Secondary ion mass spectrometry (SIMS) was previously done on some of the samples in this set (Solomon et al., 1989). Holmium was found in the InP:Ho samples tested with SIMS, therefore, holmium must not become optically active in these InP samples. There can be several possible reasons for a signal not being detected. One obvious reason could be that signals may be too weak to detect with the present experimental setup. Another possible reason could be that the above bandgap excitation is simply not transfered to the holmium 4f shell.

Spectra for the conventionally annealed samples are shown in Figure 9, while those of the RTA samples are shown in Figure 10. The only sharp peaks observed are those in the conventional 750°C, 15 minute annealed sample. This peak at 1.377 eV and its accompanying lower energy peak at 1.334 eV have been attributed to near-edge emissions. The main peak is due to a combination of free-to-bound acceptor and donor-acceptor transitions involving unknown impurities (Oberstar and Streetman, 1982; Pomrenke et al., 1981). The smaller peak is separated from the main peak by the energy of the longitudinal optical (LO) phonon, .043 eV (Oberstar
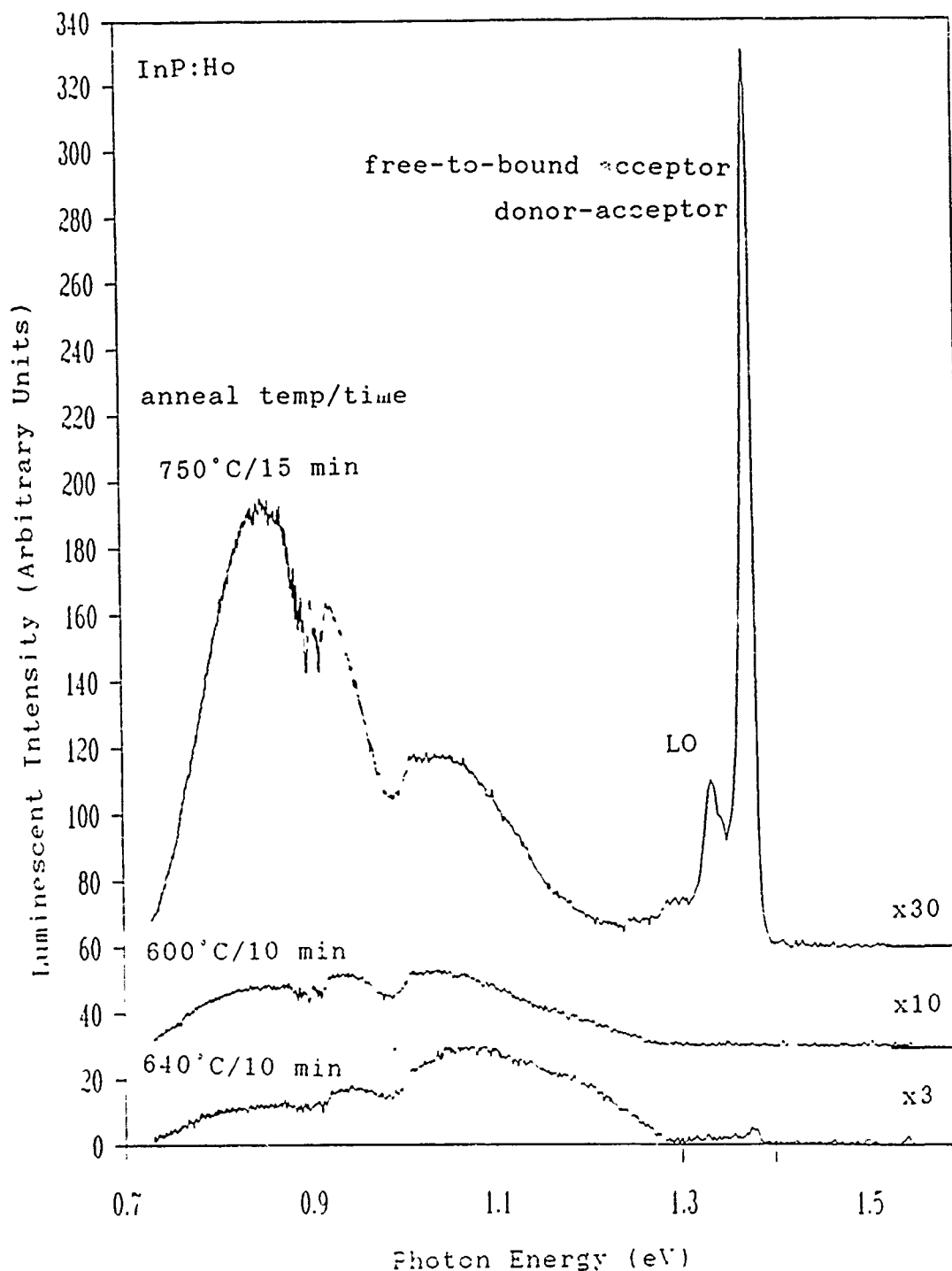
34

Figure 9. Comparison Spectra of InP:Ho samples annealed by the Conventional Furnace Method. The Uppermost Spectra is a 100 keV Holmium Implant Recorded with a 500 μm spectrometer slit opening. The Lower Two are 1000 keV Holmium Implants Recorded with a 300 μm Slit.
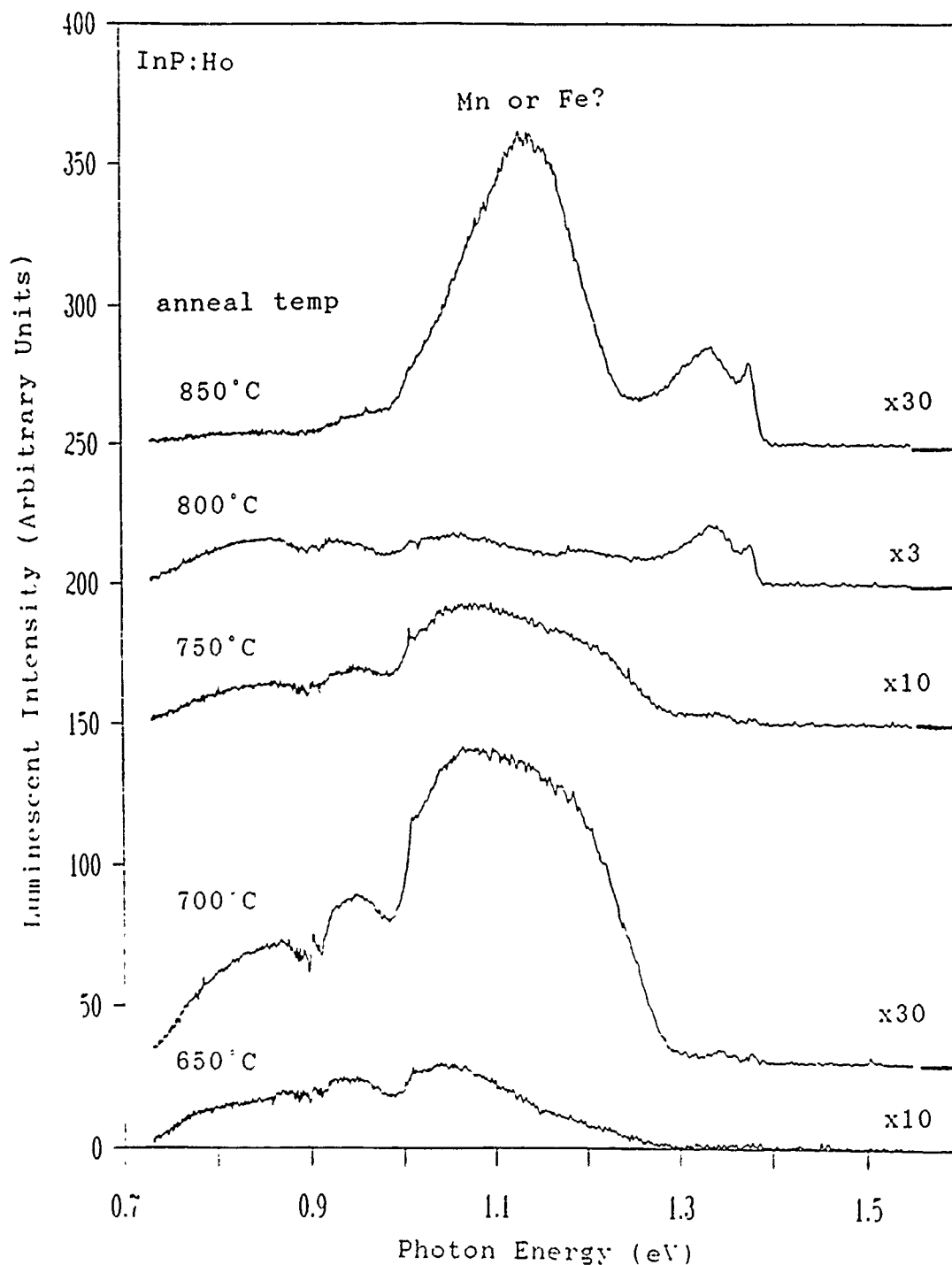
Figure 10. Comparison Spectra of InP:Ho Samples Annealed by the Rapid Thermal Method for 15 Seconds. The 800°C and 700°C Annealed Samples were Examined with a 500 μm Spectrometer Slit Opening, While the Others were Examined with a 300 μm Slit Opening.

and Streetman, 1982:5155), and is therefore a phonon replica. All three conventionally annealed samples show broad emissions which are most likely related to crystal damage caused by implantation.

The RTA samples show a trend as anneal temperature is increased. All RTA samples were annealed for 15 seconds. The 650°C annealed sample shows very broad emissions from .7 to 1.24 eV. In the case of the 700°C annealed sample, the emissions from .7 to 1.0 eV begin to quench, while those from 1.0 to 1.24 eV increase in intensity. The 750°C annealed sample continues this trend, but the overall intensity decreases. At an anneal temperature of 800°C, sharp near-edge emissions begin to appear between 1.36 and 1.38 eV. Finally, in the 850°C annealed sample, the near-edge emissions are more well-defined and a strong broad band is seen centered around 1.13 eV. The broad band is possibly related to manganese and iron contaminants in the samples. At least one study (Eaves et al., 1982) has shown that manganese and iron are common contaminants. Both impurities give rise to broad emissions in the 1.1 eV region which become more pronounced upon annealing.

A plausible explanation for the observed trend in luminescence with anneal temperature concentrates on lattice damage. The high energy implantation of holmium atoms causes lattice damage which would lead to many types of defect-related luminescence. Annealing repairs this damage

37

and restores the sample to a more perfectly crystalline state. Higher anneal temperature would allow the atoms in the sample greater ability for motion. Therefore, at 800°C and 850°C anneal temperatures, near-edge emissions of the type seen in a perfect crystal begin to appear. Also, subsequent loss of defect related emissions occurs.

Si:Ho

Spectra were taken of three 1000 keV holmium-implanted silicon samples. These samples were all n-type having been doped with phosphorus. In the region of interest for holmium, the near-edge to 1.04 eV (1.19 μm), six peaks were observed in 4.2 K spectra (Figure 11), but only three peaks were found in 25 K spectra. Those peaks were at different energy locations (Figure 12). Holmium 4f emissions should not shift with temperature and therefore any of the observed peaks were not believed to be holmium related. The most convincing evidence that the observed luminescence was not holmium related was obtained by examining an unimplanted n-type silicon sample. The unimplanted sample showed the same series of six peaks at 4.2 K, thereby confirming that these peaks were not holmium related.

To understand the origin of the 25 K peaks, the phosphorus doping must be considered. Dean et al. (1967) observed similar spectra for phosphorus-doped silicon. The three most intense peaks recorded at 26 K by these authors
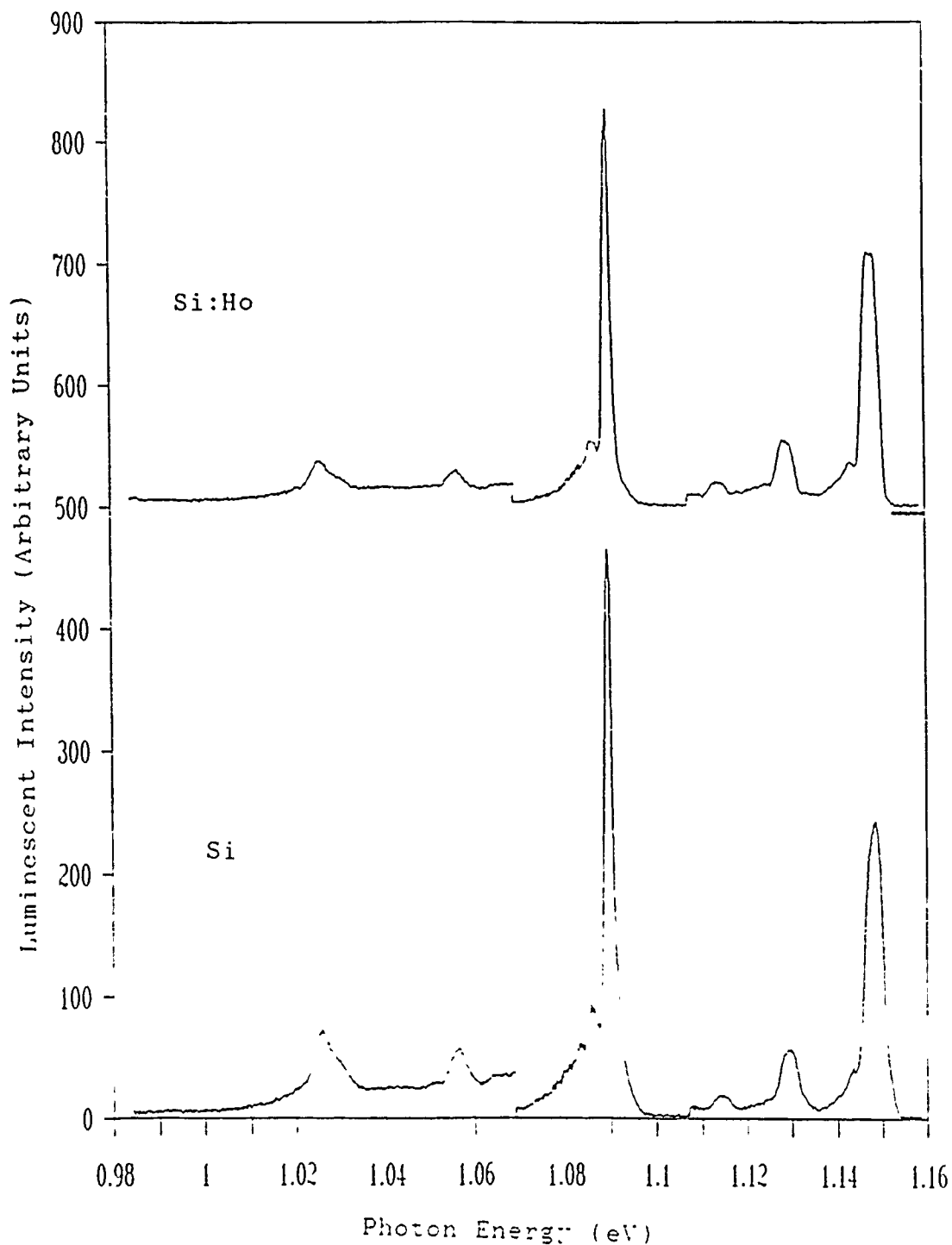
38

Figure 11. Comparison at 4.2 K of Holmium Implanted Silicon (upper spectra) and Unimplanted Silicon (lower spectra). The 1.069 to 1.104 eV Region was Recorded with a 500 μm Spectrometer Slit Opening, While the Remaining Regions were Examined with a 1000 μm Opening.
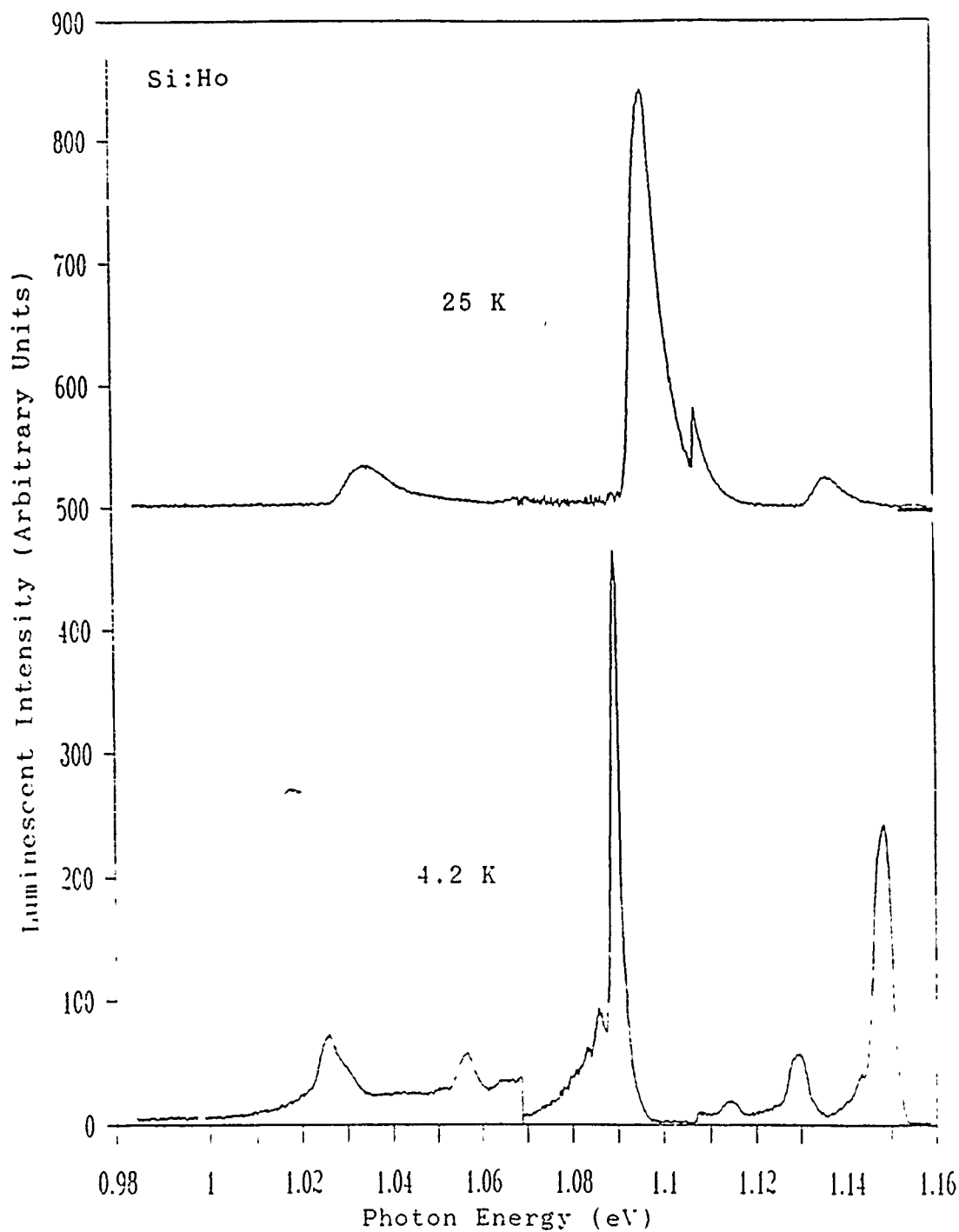
Figure 12.   Comparison of 25 K (upper spectra) and 4.2 K
(lower spectra) Spectra of Holmium Implanted Silicon Sample
Annealed at 750°C for 15 Minutes.   The 1.069 to 1.104 eV
Region was Recorded with a 500 μm Spectrometer Slit Opening,
While the Remaining Regions were Examined with a 1000 μm
Opening.

40

coincide closely with observations made in this study (Table 5). They attribute these peaks to free-exciton emissions.

TABLE 5
Silicon 25 K and 26 K Emissions

Observed Maxima(eV) at 25 K	Threshold(eV) at 26 K (Dean et al.)	Assignment (Dean et al.)
1.0339	1.0325	FE-TO(MC)-ZC
1.0961	1.0970	FE-TO(MC)
1.1360	1.1365	FE-TA(MC)

FE = Free Exciton emission 1.1548 eV
TO = Transverse Optical Phonon .0578 eV
TA = Transverse Acoustic Phonon .0183 eV
ZC = Zone Center Optical Phonon .0645 eV

All free-exciton peaks must be accompanied by phonons to conserve momentum in indirect band gap transitions. Quoted values for the phonon energies are 57.8 meV for the transverse optical (TO) phonon, 18.3 meV for the transverse acoustic (TA) phonon, and 64.5 meV for the optical zone center phonon (ZC). Using these phonon values and assuming a free-exciton gap of 1.1548 eV, the values shown in Table 5 were obtained.

The energy locations of the lines observed here are slightly different than those recorded by Dean et al. (1967:712) due to several factors. First, the slight difference in temperature (25 K verses 26 K) leads to a small difference in bandgap. More importantly, maxima of intensity were used as line positions in this study, whereas

41

Dean et al. used threshold energies. Threshold energies are found by fitting against Maxwell-Boltzmann (MB) intensity distributions for each line. This shape is apparent in the lines observed in this study. (See Figure 12.) The threshold energy is the minimum at which a free-exciton is formed. Since free-excitons can also have translational energy within the lattice, there is a MB distribution of energies above threshold. The distribution maximum is always greater than threshold. A final source of error was that the spectrometer reading was taken for calibration of the absolute line position. Error was estimated at less than .2 nm by comparing argon calibration lines with the spectrometer readings.

At 4.2 K, the spectrum becomes much more complicated. Excitons can now become bound to impurities. The principle bound-exciton lines observed can be attributed to phosphorus. Table 6 lists the measured energies of the peaks and compares them to the lines observed by Dean et al. (1967:717). Since the excitons were now bound and therefore had no translational energy, the MB line shape was no longer observed. Binding of excitons also lowered the energy by E_b as can be seen from comparison of FE-TO at 1.0970 eV and P-TO at 1.0916 eV. Also note that no-phonon (NP) lines were now possible, because the phosphorus atom can participate in the transition providing momentum conservation.

42

TABLE 6
Silicon 4.2 K Emissions

Observed Maxima(eV)	Dean et al. (eV)	Assignment (Dean et al.)
1.1480	1.1496	P^0
1.1291	1.1311	$P_6{}^0$
1.1143	1.116	$P_4{}^0, P_1{}^{TO}$
1.0895	1.0916	P^{TO}
1.0561	1.0580	$P_4{}^{TO}$
1.0258	1.0271	$P_5{}^{TO}$

Superscripts denote phonons (0 is a no-phonon line).
Subscripts denote the excitation state of the bound exciton.

GaAs:Ho

Spectra were taken of six GaAs:Ho samples which are listed in Table 4. Three of the samples were low energy implants of 100 keV and the others were 1 MeV implants. All samples were annealed for 15 minutes at temperatures of 750°C, 850°C, and 950°C.

The two different implant energy sample groups have luminescence which follows a similar trend with anneal temperature. (See Figures 13 and 14.) The 750°C annealed samples show strong, well-defined near-edge emissions. The 850°C annealed samples show weaker emissions, and finally, the 950°C annealed samples again show much stronger emissions.

The strong, multiple peak structure between 1.25 and 1.39 eV (1.01 and 1.11 μm) has been identified as due to copper substituting on a gallium site (Queisser and Fuller,
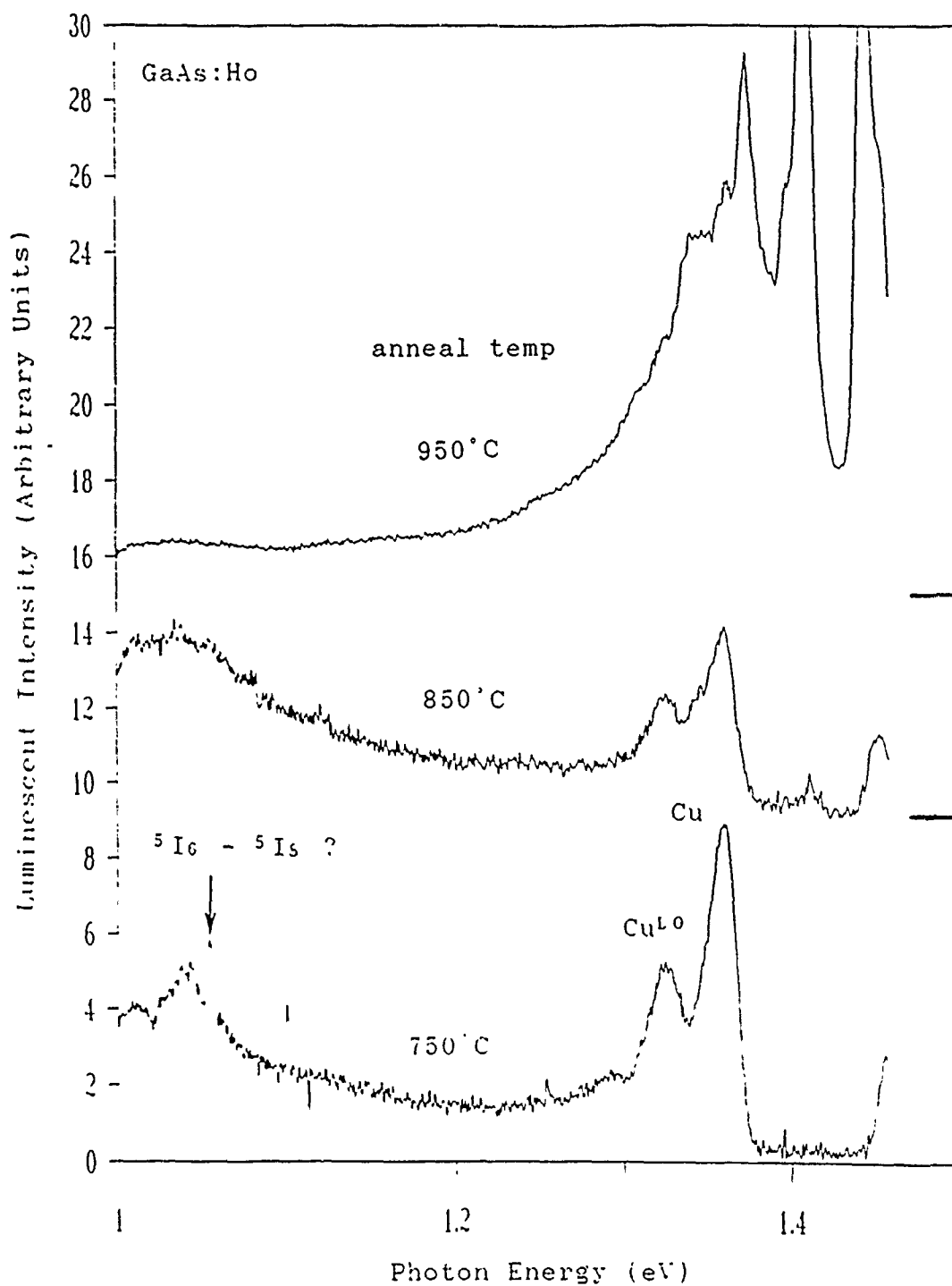
Figure 13.   Comparison of Spectra for 100 keV Holmium
Implanted GaAs Samples with Different Anneal Temperatures.
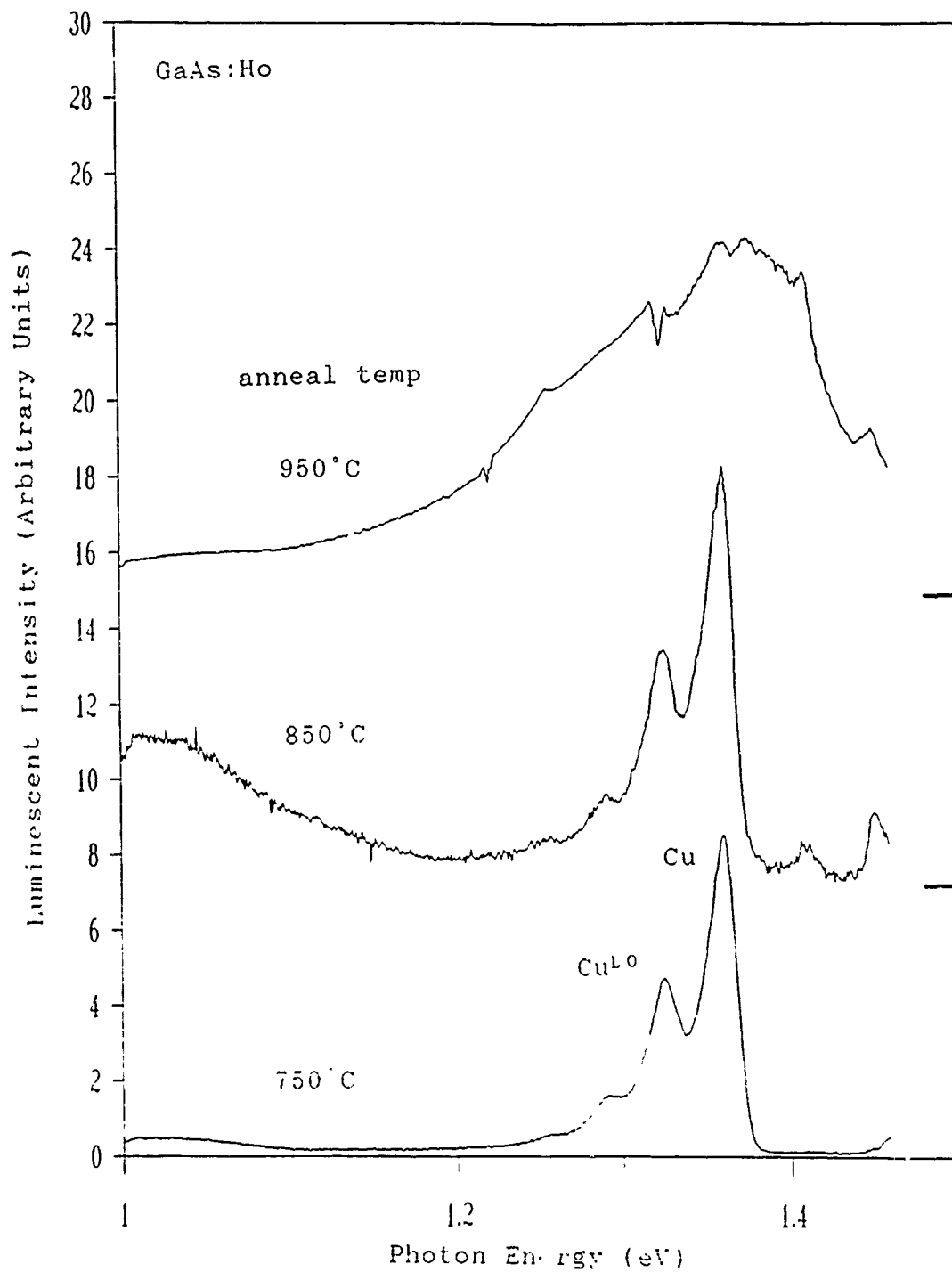All Samples were Annealed for 15 Minutes.

Figure 14. Comparison of Spectra for 1000 keV Holmium
Implanted GaAs Samples with Different Anneal Temperatures.
All Samples were Annealed for 15 Minutes.

1966:4896). The main peak which is at average energy
1.362±.005 eV in the six samples is caused by a free-to-
bound transition to the copper-acceptor level .156 eV (Wang
et al., 1985:230) from the valence band. To confirm that
this peak is indeed a copper-acceptor peak, the direct gap
of GaAs at 4.2 K was calculated using an empirical formula
relating band gap to temperature (Blakemore, 1982:R155).
This treatment gives a value of 1.5189±.0030 eV for the band
gap. The value calculated using the observed peak at
1.362±.005 eV and the known value for the copper-acceptor,
.156 eV, is 1.518±.005 eV, well within experimental error.

It is well known that the copper-acceptor couples
strongly with phonons (Queisser and Fuller, 1966:4897). The
smaller peak on average .0357±.0004 eV below the main peak,
is therefore a LO phonon replica. The accepted value for the
LO phonon is taken from a linearized form for LO energy
variation with temperature which gives .03656±.0006 eV at
4.2 K. Again, this is within error of the observed value.
The small structure sometimes visible below the replica is
most likely a 2LO replica of the main peak, but the spectra
were not of high enough resolution to accurately determine
the peak's energy.

The small peaks near 1.41 and 1.45 eV are most likely
due to other impurities or phonon replicas of other
near-edge emissions (these near-edge emissions were off the
range of the germanium detector, that is above 1.45 eV).

46

For instance, magnesium, a well known impurity in GaAs, has emissions at 1.4089 eV (Blaauw et al., 1985:664). Also, a LO replica of the free-exciton line (1.4832 eV) is located at 1.4472 eV (Wang et al., 1985: 230). This identification is only tentative, however. Since the main near-edge emissions were above the accessible range of the germanium detector and were not the emphasis of this study, they were not recorded.

Below approximately 1.18 eV (1.05 µm), a broad band emission is observed. This region also happens to be the area in which the holmium $^5I_6$-$^5I_8$ emissions would be expected. This region was studied more closely with slower spectrometer scans and wider apertures to detect any possible holmium 4f emissions. Unfortunately, only one candidate peak was observed. In the 100 keV implant, semi-insulating GaAs annealed at 750°C for 15 minutes, one peak was clear at 1.055 eV. This peak did not occur in any of the other samples, but was observed on several spectra of the original sample. To test if this result was reproducible in other samples, another GaAs:Ho 100 keV implanted semi-insulating sample was annealed at 750°C for 15 minutes. This sample did not show the 1.055 eV peak. Similar samples were also annealed at 700°C and 800°C which also did not show the peak in question. This result is unexplained. Possible reasons are a peak due to a contaminant that only affected this one sample, some unknown

defect state, or for some unknown reason, the holmium was 'activated' in this one sample.

Thulium

One focus of this study was the search for Tm^{3+} emissions in n- and p- type GaAs. AlGaAs:Tm was also examined and compared to previous results for GaAs:Tm. Finally, Si:Tm samples were tested for Tm^{3+} emissions. All samples were implanted with 390 keV thulium with a dosage of 5×10^{13} cm^{-2} ($\pm 5\%$).

Previous Work on GaAs:Tm

GaAs:Tm has been previously studied by Pomrenke (1989). For semi-insulating GaAs, emissions were found in the .93 to 1.03 eV (1.2 to 1.35 μm) region and were attributed to 4f-4f transitions be ween the spin-orbit levels $^3H_5$ -$^3H_6$. Since only semi-insulating GaAs was investigated previously, n- and p- type GaAs were examined in this study.

Pomrenke (1989:166) also found an anneal temperature of 725°C to be optimum for maximizing the Tm^{3+} emissions in GaAs. Also noted was a possible change in the type of thulium center responsible for the emissions. At an anneal temperature of 600°C, the relative intensities of the Tm^{3+} lines changed, indicating that the crystal field experienced by Tm^{3+} must have changed. Such an occurrence would be

48

expected if implanted ions were located interstitially, but upon annealing, moved to a lattice site. The fall off in intensity of the Tm^{3+} emissions at anneal temperatures higher than 725°C could be due to quenching by other impurities. Even if the Tm ions were immobile (perhaps on lattice sites), other impurities may become mobile at higher temperatures forming complexes with the Tm^{3+} and thereby quenching the luminescence.

Pomrenke (1989) performed a temperature dependence study on the 4f emissions of a 750°C ten minute annealed, encapsulated GaAs sample. It was found that the Tm^{3+} emissions were sharp, frequency stable lines up to about 166 K. At higher temperatures, the intensity rapidly falls off and the lines disappear into the background. Also noted was a so-called 'hot' line at 1.024 eV (1.208 μm). This emission did not appear until temperatures were above 42 K. This line is interpreted as being due to thermal excitations of a higher line within the upper spin-orbit level than that which is responsible for the 6 K emissions.

n- and p- Type GaAs:Tm

Both n- and p- type GaAs samples were studied to determine whether Tm^{3+} 4f-4f emissions were present. The samples examined are listed in Table 7. No Tm^{3+} emissions were observed for any of these samples in the .93 to 1.03 eV (1.2 to 1.35 μm) region. Figure 15 shows the Tm^{3+} $^3H_5$ -$^3H_6$
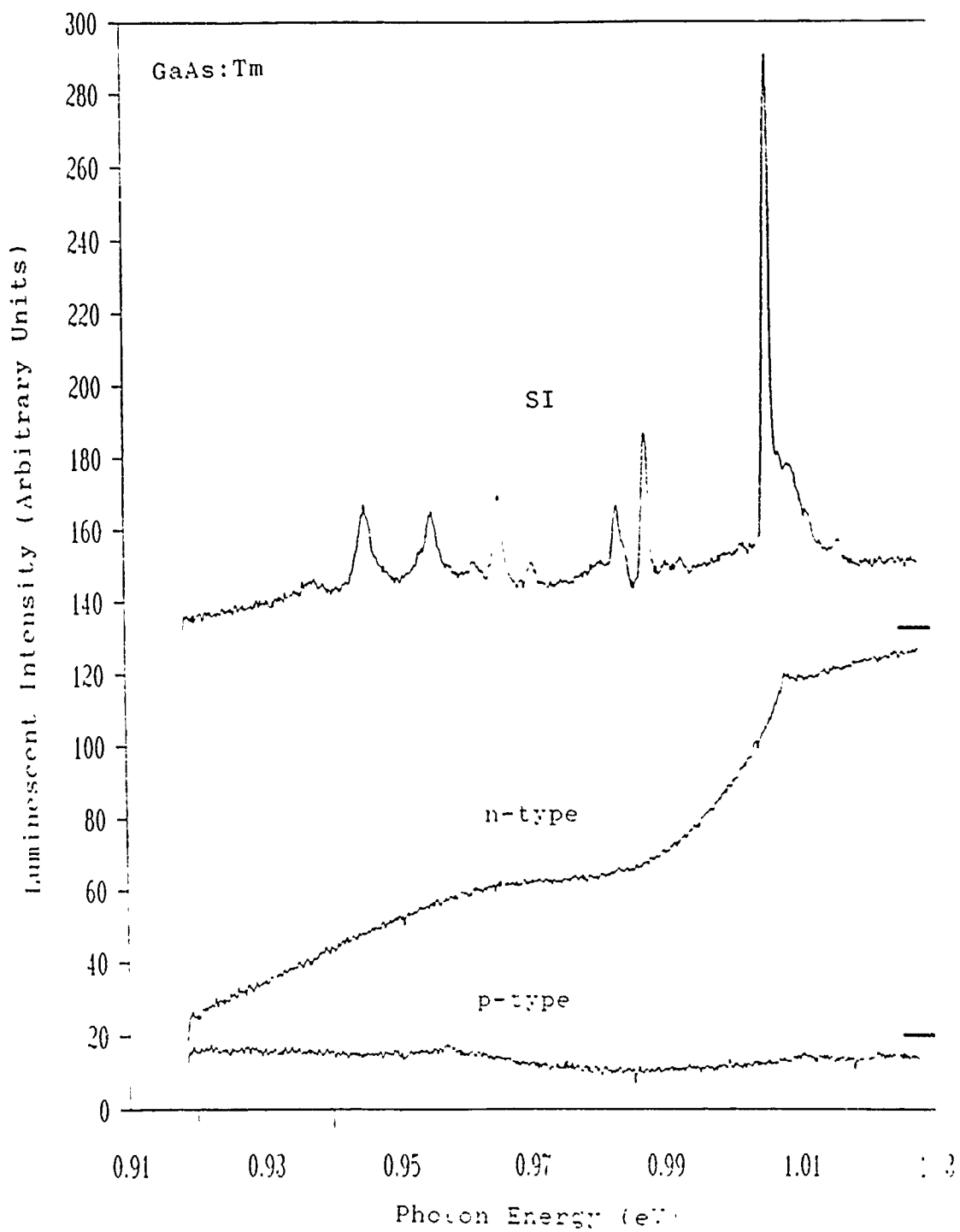
49

Figure 15. Comparison Spectra of p-type, n-type, and Semi-Insulating GaAs.

emissions in GaAs and the corresponding spectral regions in n-type and p-type GaAs. The n-type GaAs shows a curious background signal which may mask the thulium signal. Since 4f emissions are not seen in either n- or p- type GaAs, heavy doping with impurities must interfere with 4f excitation or lead to non-radiative 4f decay.

AlGaAs:Tm

This study concentrated on a small set of $Al_x Ga_{1-x} As$ as shown in Table 8. One of the GaAs samples examined by Pomrenke (1989) was also included for comparison purposes.

TABLE 7
GaAs:Tm n- and p- Type Samples

COND TYPE	DOPANT	ANNEAL TEMP/TIME/GAS
p	Zn	725°C/15 min/N$_2$
p	Zn	775°C/15 min/N$_2$
p	Zn	825°C/15 min/N$_2$
n	Si	650°C/15 min/N$_2$
n	Si	700°C/15 min/N$_2$
n	Si	750°C/15 min/N$_2$

TABLE 8
AlGaAs:Tm Implanted Samples

SAMPLE	ANNEAL TEMP/TIME/GAS
Al.$_{15}$Ga.$_{85}$As	600°C/10 min/fg
Al.$_{15}$Ga.$_{85}$As	675°C/10 min/fg
Al.$_{15}$Ga.$_{85}$As	750°C/10 min/fg
Al.$_{23}$Ga.$_{77}$As	825°C/15 min/fg

Figure 16 shows spectra of each AlGaAs sample in the
.93 to 1.03 eV (1.2 to 1.35 μm) range. First, note that for
the x=.15 samples a similar trend to that in GaAs is seen.
The 675°C and 750°C annealed samples show the same series of
peaks, while the 600°C annealed sample differs considerably.
There seem to be as many Tm^{3+} peaks in the 600°C annealed
sample, but the energetic spacings and absolute energy
locations have changed. Also note that as for GaAs the
750°C annealed sample has more intense emissions than the
675°C annealed sample. The one x=.23 sample only showed one
weak peak centered at 1.01 eV (1.23 μm).

Figure 17 shows a comparison spectra of the 750°C, 15
minute annealed AlGaAs sample with the best GaAs sample, a
725°C, 15 minute annealed sample. The AlGaAs sample shows
the same series of peaks as in GaAs and they are located at
the same energetic positions. The numerous peaks seen were
all due to transitions between the $^3H_5$ to $^3H_6$ spin-orbit
levels. Only one transition energy would be seen in the
free ion, but the crystalline environment of the ion causes
this transition to split into many levels.

If we assume for the moment that only one type of Tm^{3+}
center is present then all lines would be due to this
center. Also, if we further assume that only transitions
from the lowest $^3H_5$ level occur, then all of the crystal
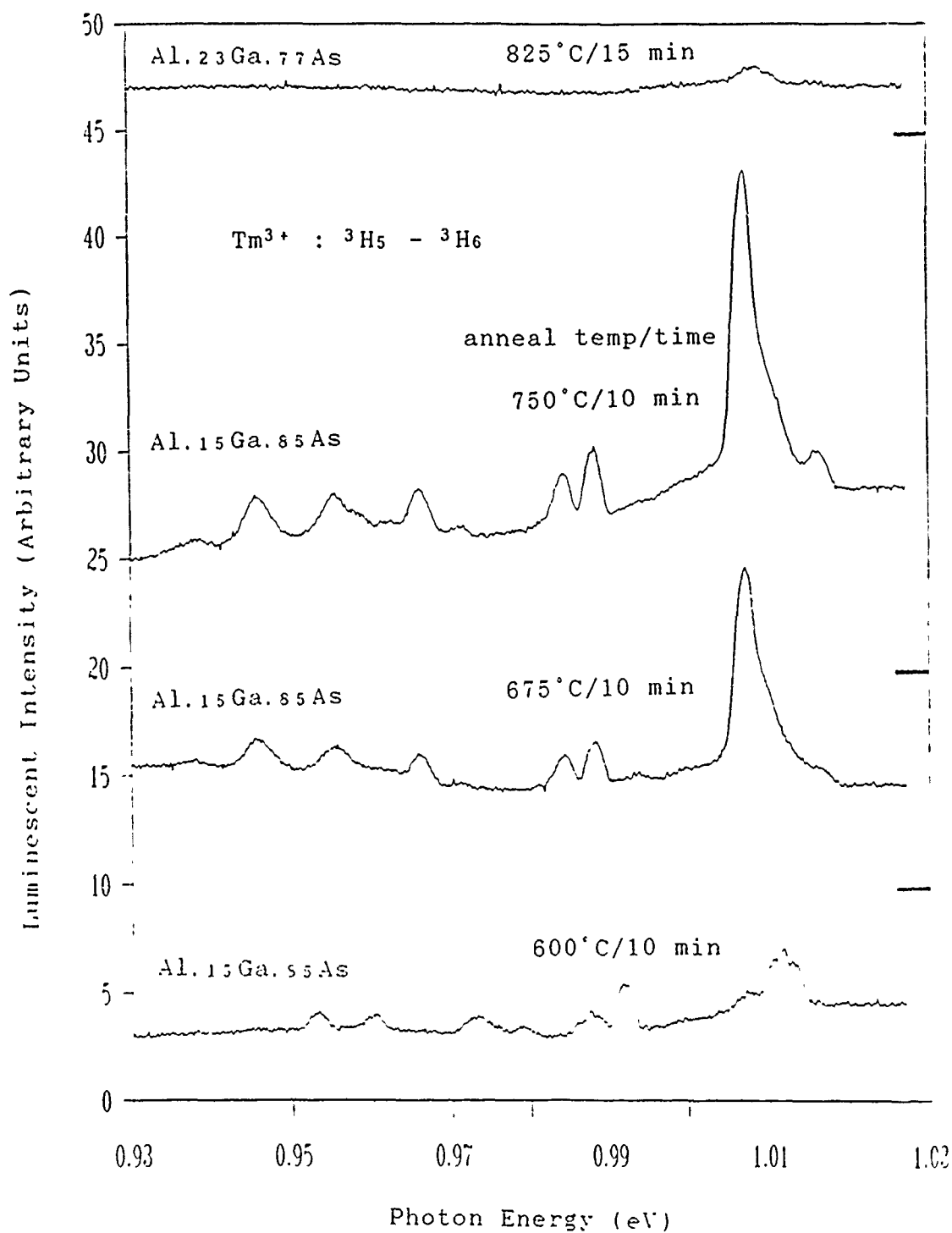field splitting is in the $^3H_6$ manifold of states. This

52

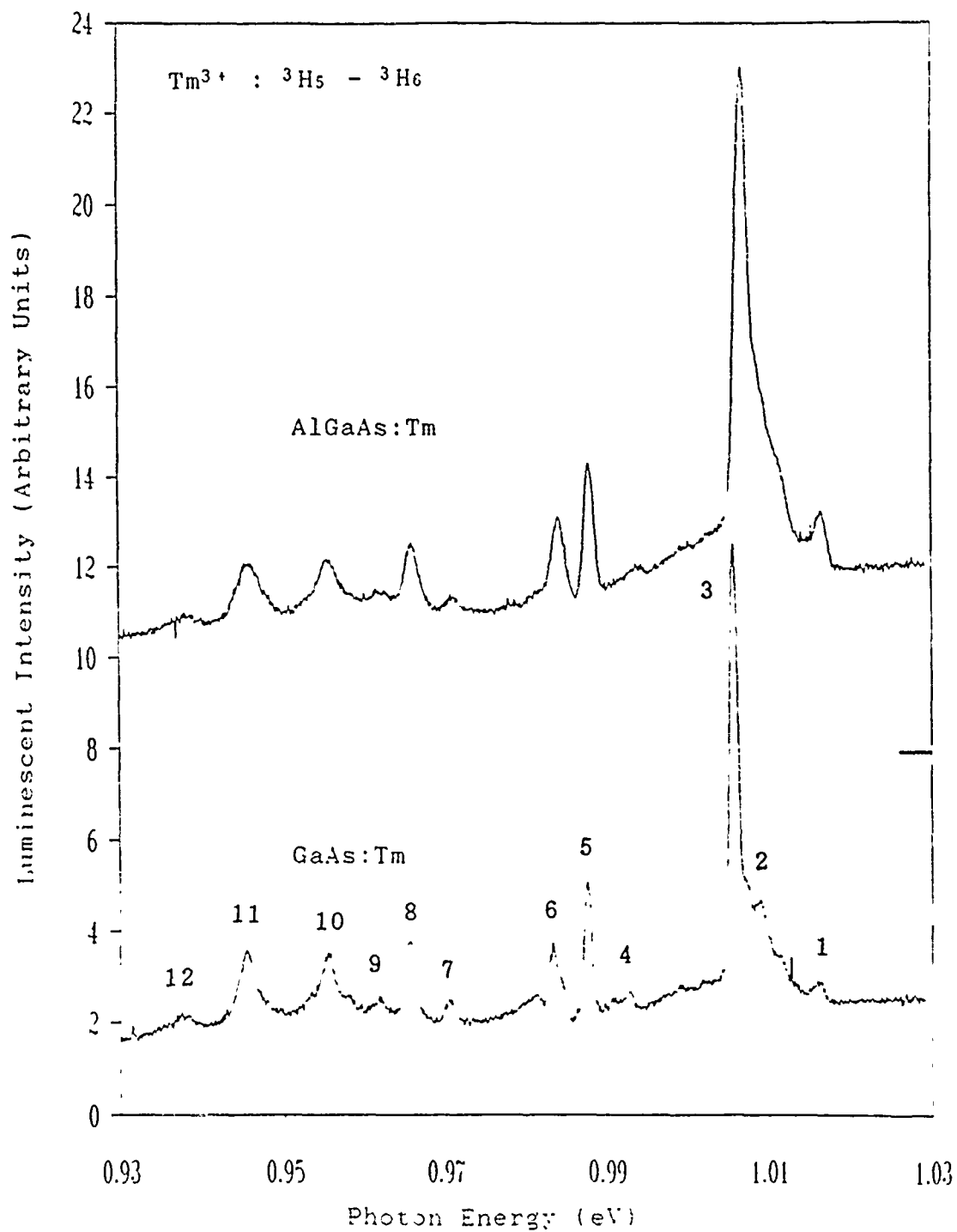Figure 16. AlGaAs:Tm Sample Comparison Spectra Showing Tm^{3+} Emissions.

Figure 17. Comparison of Spectra of 390 keV Thulium Implanted in $Al_{.15}Ga_{.85}As$ Annealed for 15 min at 725°C with GaAs Annealed for 10 min at 750°C.

54

assumption would be justified if non-radiative processes allowed higher $^3H_5$ states to decay to the lowest $^3H_5$ state. It has been shown that for the J=6 state, as is the case for $^3H_6$, the state will split into six levels in a field of cubic symmetry, ten levels in a field of tetragonal symmetry, and a maximum of thirteen levels in a field of lower symmetry (Walter, 1984:405). On the basis of these assumptions and knowing that there are at least eight strong peaks in the spectrum, one can conclude that the site occupied by Tm^{3+} is of lower than cubic symmetry. If the site were of less than cubic symmetry, then the Tm^{3+} would not be substitutional in the lattice unless it distorted the lattice or complexes were formed.

Other explanations for the number of lines are possible. First, higher levels within the $^3H_6$ state may decay radiatively to the $^3H_5$ manifold. Second, some lines could be phonon replicas. This possibility is doubtful, however, since none of the line spacings seem to match the values of the LO and TO phonons at .003689 and .003490 eV respectively in $Al_{.15}Ga_{.85}As$ (Adachi, 1985:R8).

Temperature dependence studies were performed on the $Al_{.15}Ga_{.85}As$ 750°C and 600°C annealed samples. The results are shown in Figures 18 and 19. In both cases the Tm^{3+} lines are sharp and stable, but decrease in intensity as temperature rises. The lines stay visible over 200 K with only a faint remnant apparent at 240 K. Contrasting this
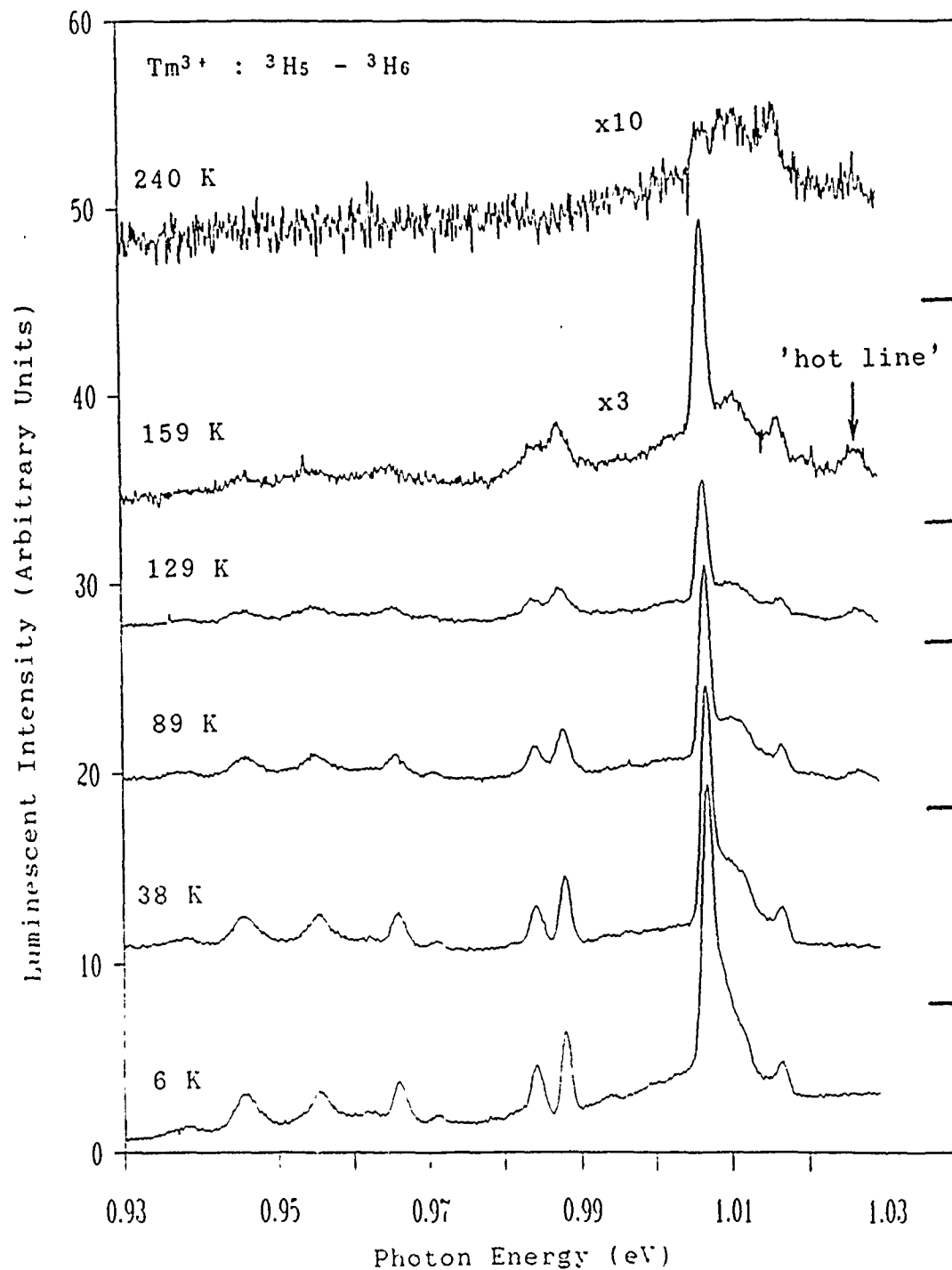
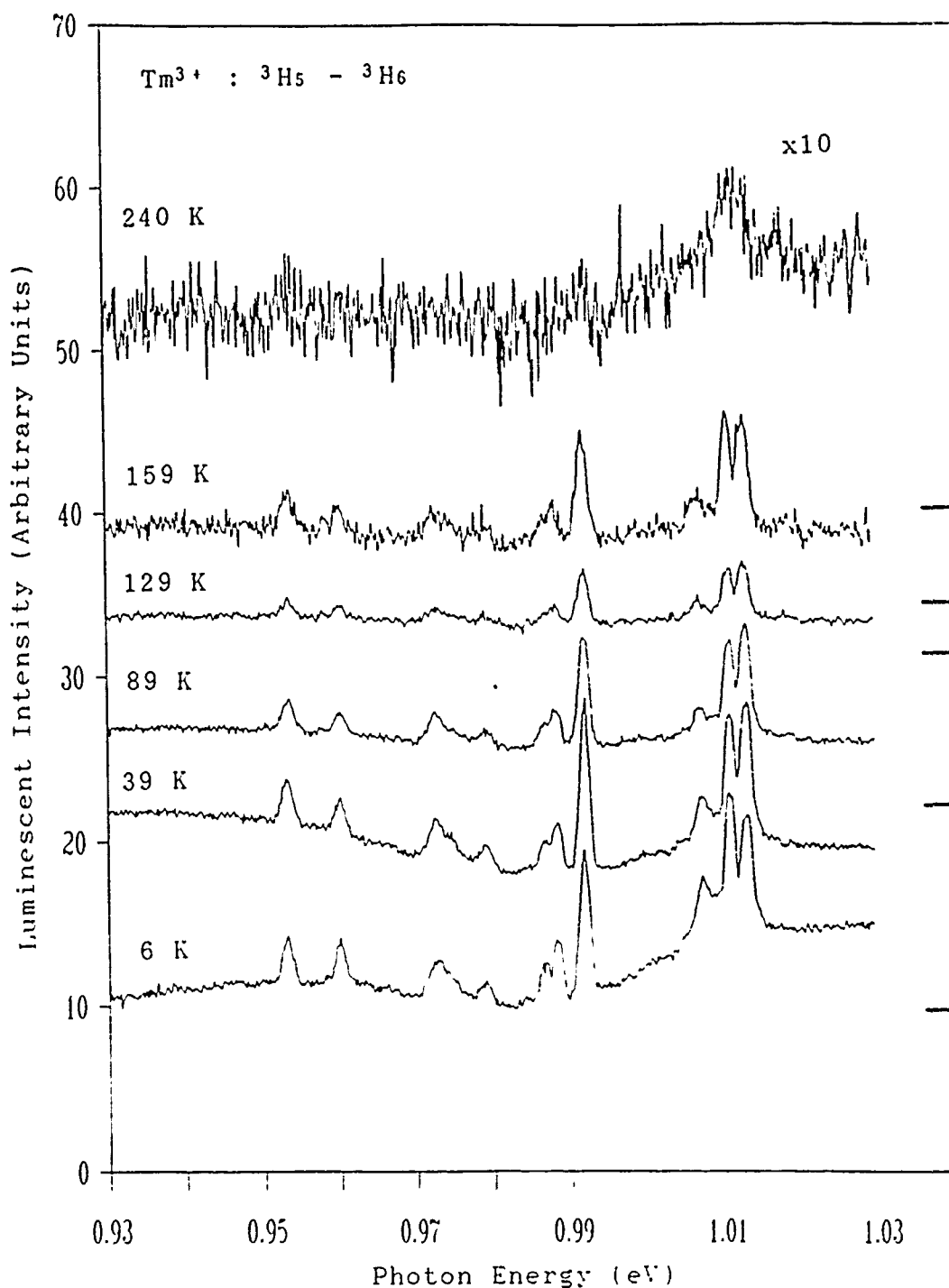Figure 18. Spectra of 390 keV Thulium Implanted Al.15Ga.85As Sample Annealed for 10 min at 750°C as a Function of Sample Temperature.

Figure 19. Spectra of 390 keV Thulium Implanted Al.$_{15}$Ga.$_{85}$As Sample Annealed for 10 min at 600°C as a Function of Sample Temperature.

57

result with GaAs shows that Tm^{3+} peaks in AlGaAs persist for over 40 K higher in temperature.

In the 750°C annealed sample, one 'hot' line is visible. The line appears in the 89 K spectra and increases in intensity relative to the other lines in the 129 K and 159 K spectra. This line quenches with all the others at higher temperature. The position of the 'hot' line is 1.026 eV (1.208 μm). This result is very similar to the behavior observed by Pomrenke (1989:172) as discussed earlier. The 'hot' line observed in that study appeared at temperatures over 42 K and was located at 1.024 eV (1.211 μm).

Excitation power dependence studies were performed on the $Al_{.15}Ga_{.85}As$ 750°C and 600°C annealed samples. Since Pomrenke (1989) did not do a similar study for GaAs, an excitation power dependence study was performed on the GaAs 725°C 15 minute annealed sample for comparison. Spectra are shown in Figures 20, 21, and 22.

To perform this study, the laser power was measured just prior to entering the sample chamber. Losses were estimated at four percent on each of the sample chamber windows. The peak intensity of the main Tm^{3+} line at 1.007 eV (1.231 eV) was then plotted verses the square root of power on target for the 750°C annealed $Al_{.15}Ga_{.85}As$ and 725°C annealed GaAs samples. (See Figures 23 and 24.) The 600°C annealed showed three strong lines and therefore all

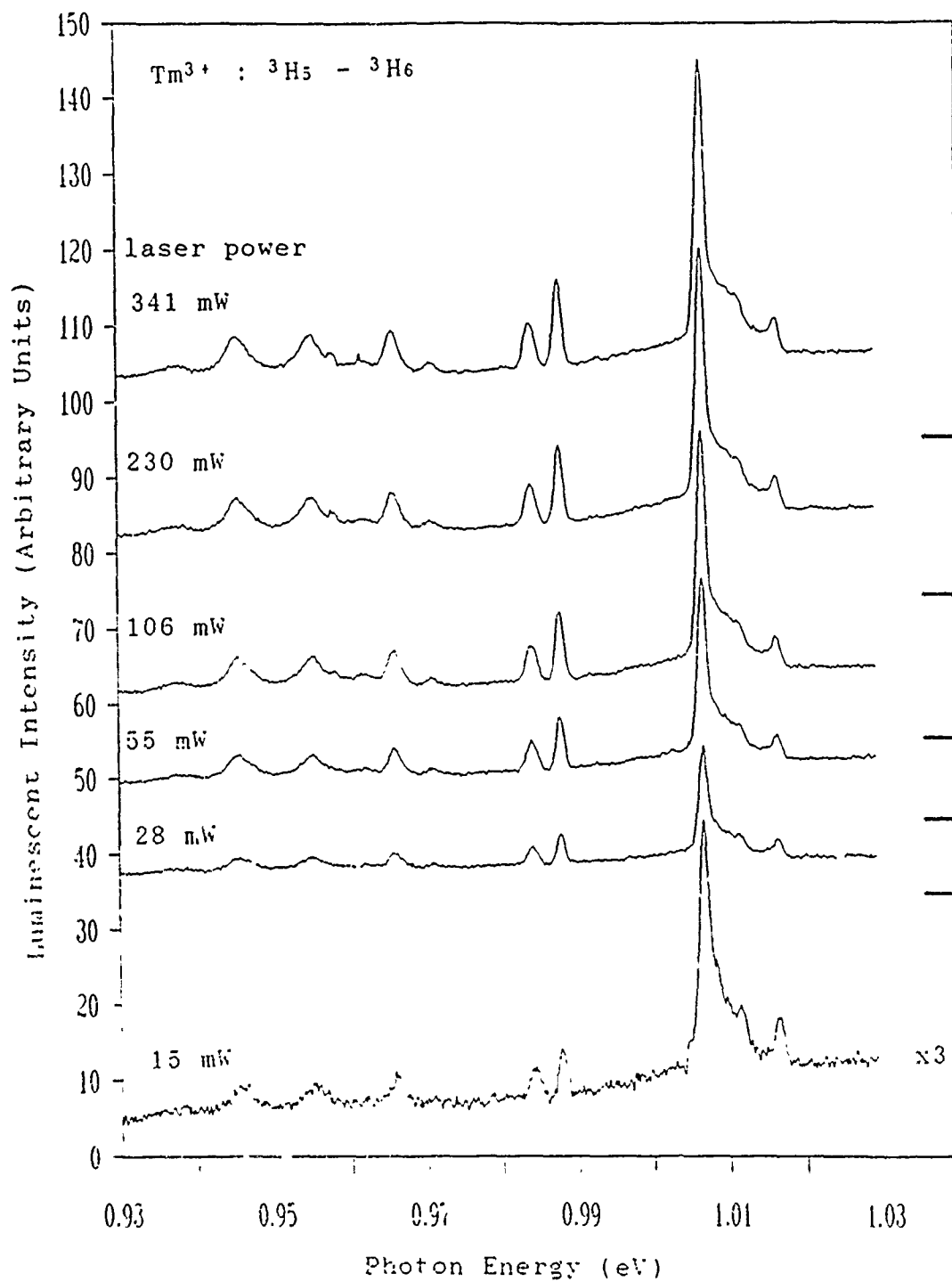Figure 20. Laser Excitation Power Dependence Study of 390 keV Implanted Thulium in $Al_{.15}Ga_{.85}As$ Sample Annealed for 10 min at 750°C.
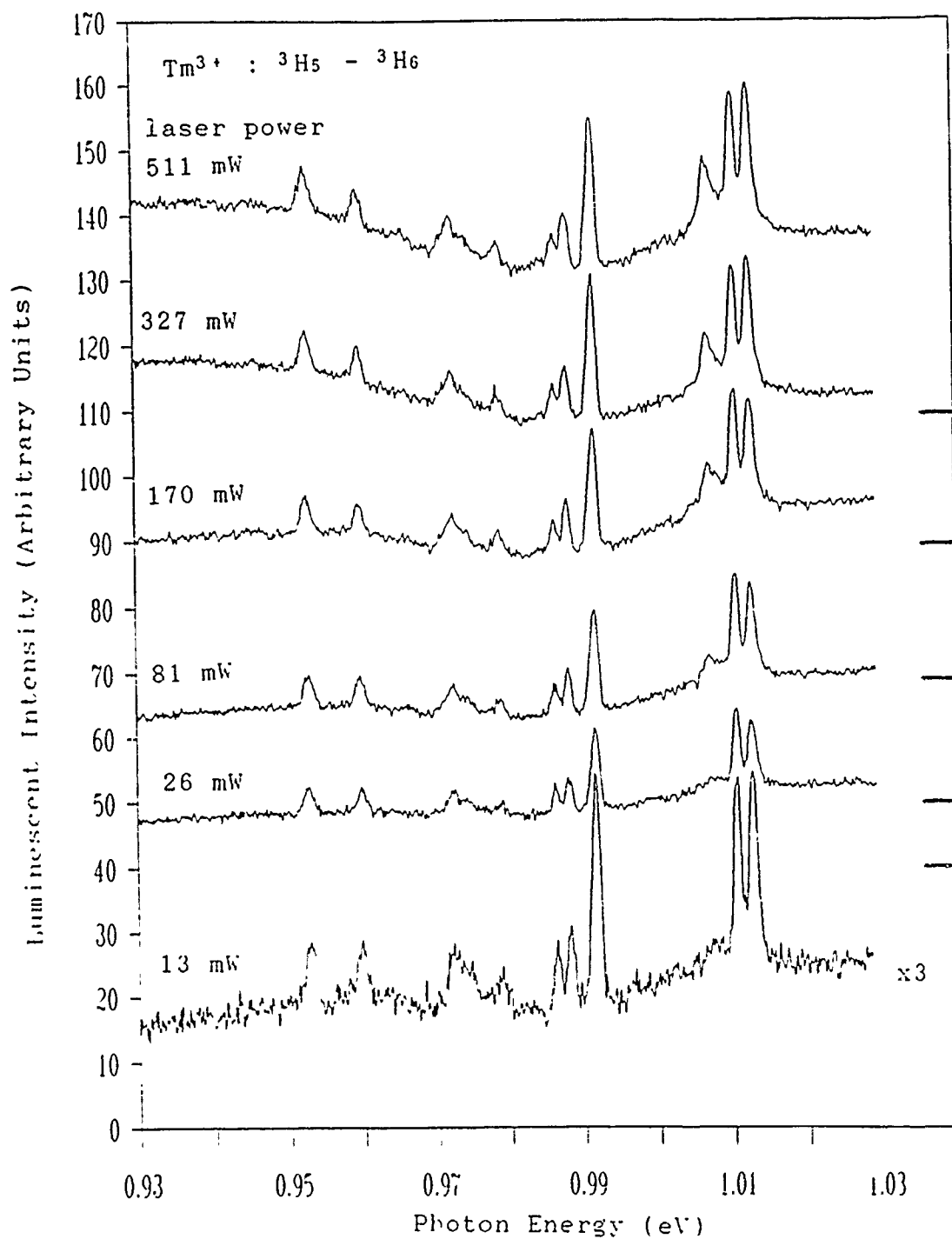
Figure 21. Laser Excitation Power Dependence Study of 390 keV Implanted Thulium in Al.₁₅Ga.₈₅As Sample Annealed for 10 min at 600°C.
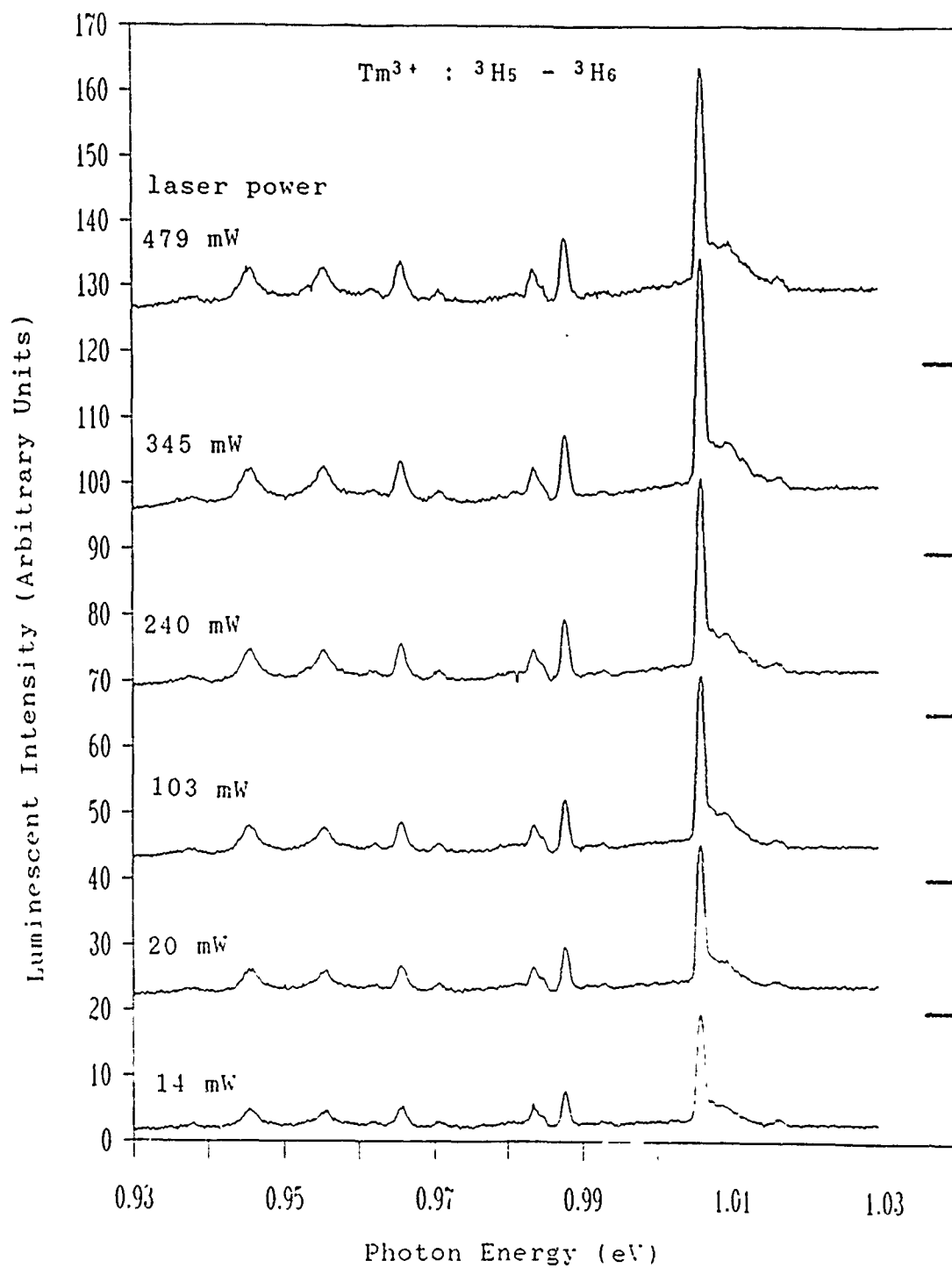
Figure 22. Laser Excitation Power Dependence Study of 390 keV Implanted Thulium in GaAs Sample Annealed for 15 min at 725°C.
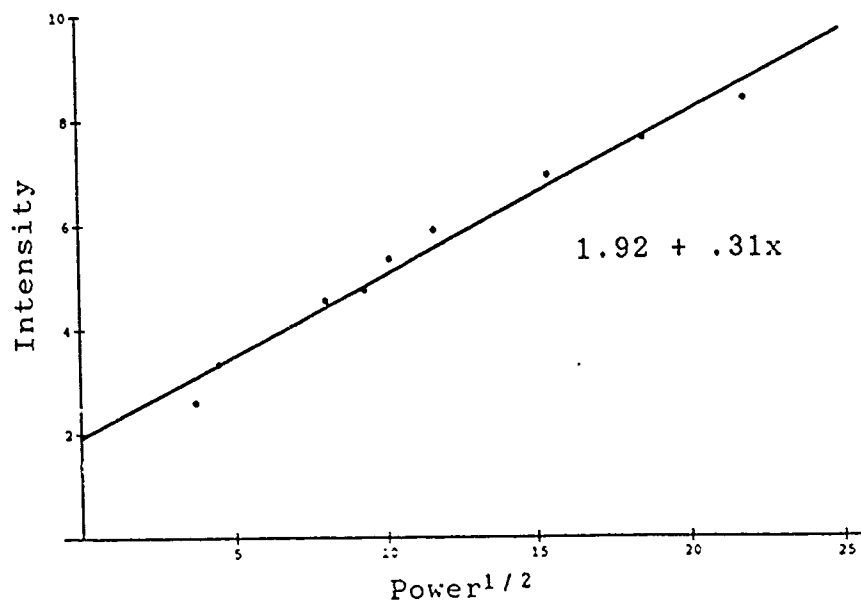
61

Figure 23. Plot of Excitation Laser Power Dependence of the 1.007 eV Line in Al$_{.15}$Ga$_{.85}$As 750°C, 10 Minute Annealed Sample Showing a Least Squares Data Fit.
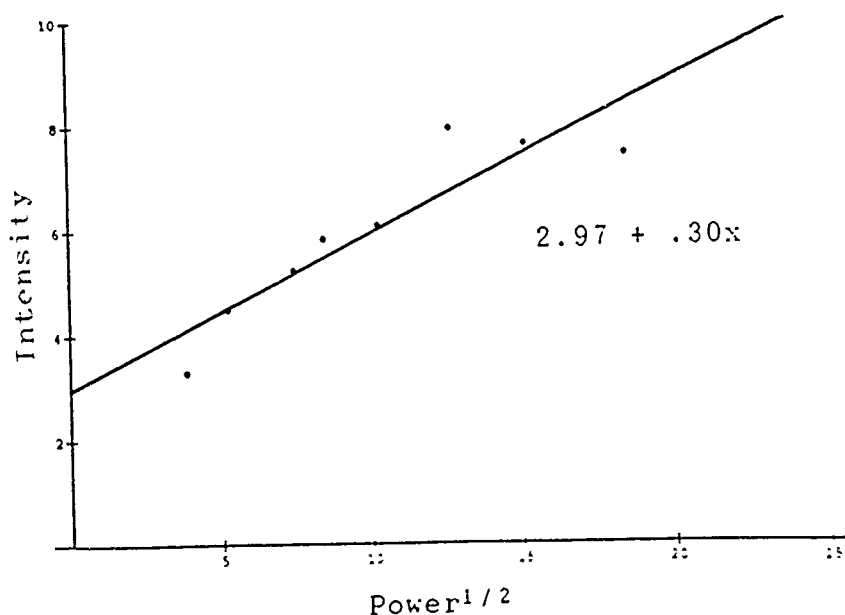

Figure 24. Plot of Excitation Laser Power Dependence of the 1.007 eV Line in GaAs 725°C, 15 Minute Annealed Sample Showing a Least Squares Data Fit.

three had peak intensity plotted as a function of square root of laser power. (See Figure 25.)

All five plots show a sublinear relationship. In fact, the lines shown on the plots are least squares fits of intensity to square root of laser power. It is clear that the square root dependence fits reasonably well, but fluctuations in peak intensity can be high. Also clear is that at lower power, the square root dependence begins to fail. Low power data points fall below the least squares fitted line, indicating a steeper than square root rise.

The observed near linear relationship between intensity and square root of excitation power was predicted by one model of RE excitation. Benyattou et al. (1990) developed a model for erbium in AlGaAs which accounts for the square root dependence found in $Al_{.45}Ga_{.55}As:Er$. In this model, excitons are created by the excitation laser source and they can transfer their energy non-radiatively by Auger recombination (transfer to free charge carriers) or to erbium ions. This model predicts that for high excitation powers:

$$n_e = C \; P^{1/2} \qquad\qquad (9)$$

where n_e is the density of excited erbium ions, C is a constant, and P is the laser power. Takahei et al. (1988) also observed a sublinear dependence of power with RE
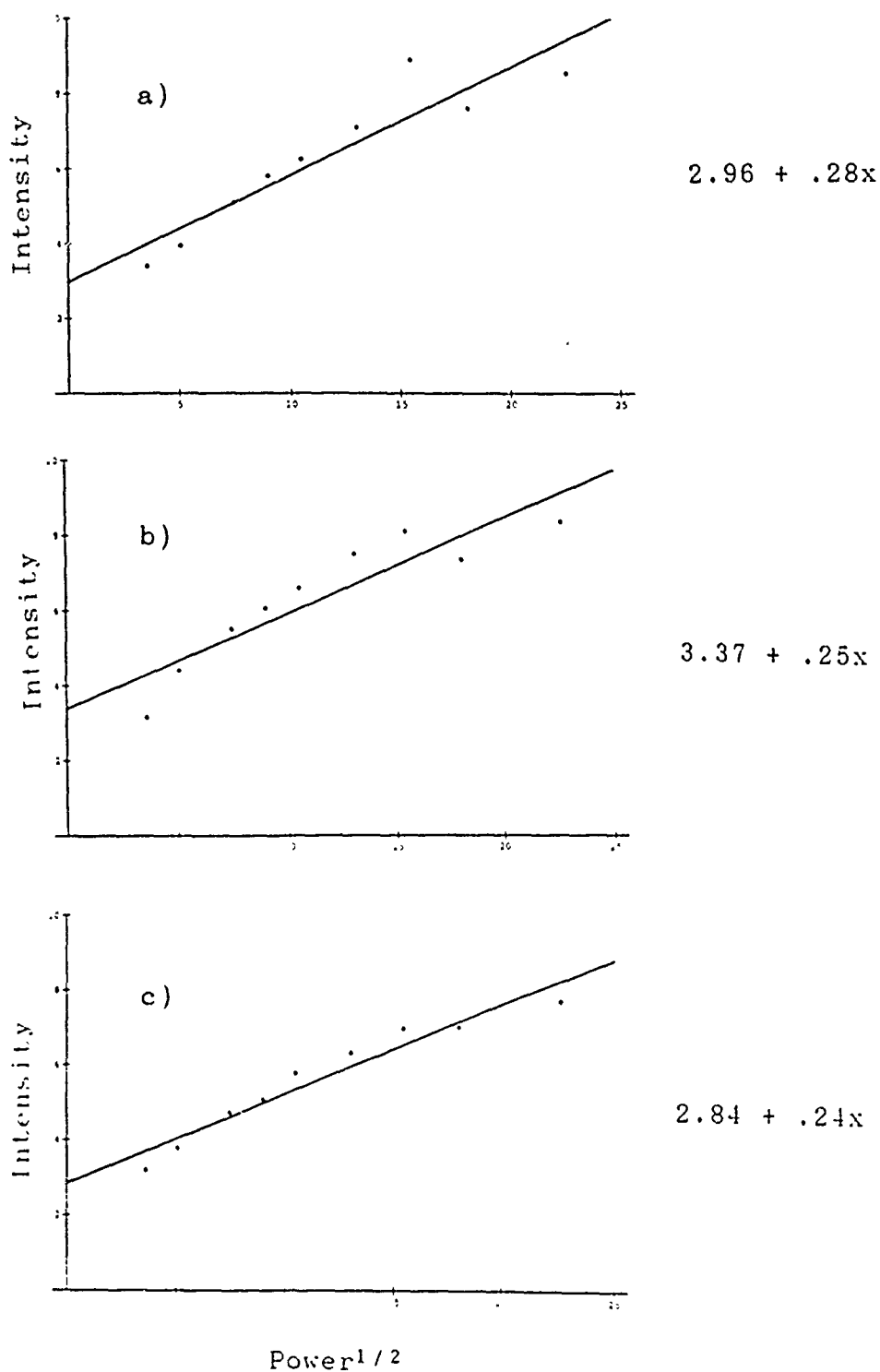
63

a)

2.96 + .28x

b)

3.37 + .25x

c)

2.84 + .24x

$Power^{1/2}$

Figure 25. Plot of Excitation Laser Power Dependence of the 1.018 eV (a), 1.015 eV (b), and .996 eV (c) Lines in $Al_{.15}Ga_{.85}As$ 600°C, 10 Minute Annealed Sample Showing Least Squares Data Fits.

intensity in InP:Er. Their result was attributed to the mostly non-radiative decay of the RE luminescence (which is manifested in decay times, 12 µs for Yb, an order of magnitude shorter than in RE doped II-VI compounds). Since the same dependence of luminescent intensity on laser power was found in this study, it may indicate a common excitation mechanism occurring in AlGaAs:Tm, GaAs:Tm, and AlGaAs:Er and possibly other REs as well.

Si:Tm

A small number of Si:Tm samples were examined for Tm^{3+} 4f emissions in the .93 to 1.03 eV (1.2 to 1.35 µm) region. The sample list is shown in Table 9.

<div align="center">

TABLE 9
Si:Tm Implanted Samples

</div>

COND TYPE	DOPING	ANNEAL TEMP/TIME/GAS	VENDOR
n	?	750°C/15 min/N_2	Wacker
p	B	750°C/15 min/N_2	Reticon
SI	-	850°C/15 min/H_2	MW
SI	-	850°C/15 min/H_2	Wacker
SI	-	850°C/15 min/H_2	Wacker (no Tm implant)

Both the n- and p- type samples showed no Tm^{3+} 4f emissions as was the case for GaAs. One of the undoped silicon (Wacker) samples did show such emissions, while the other (MW) did not. The Tm^{3+} emissions are shown in Figure 26. The thulium emissions are shown by arrows and are
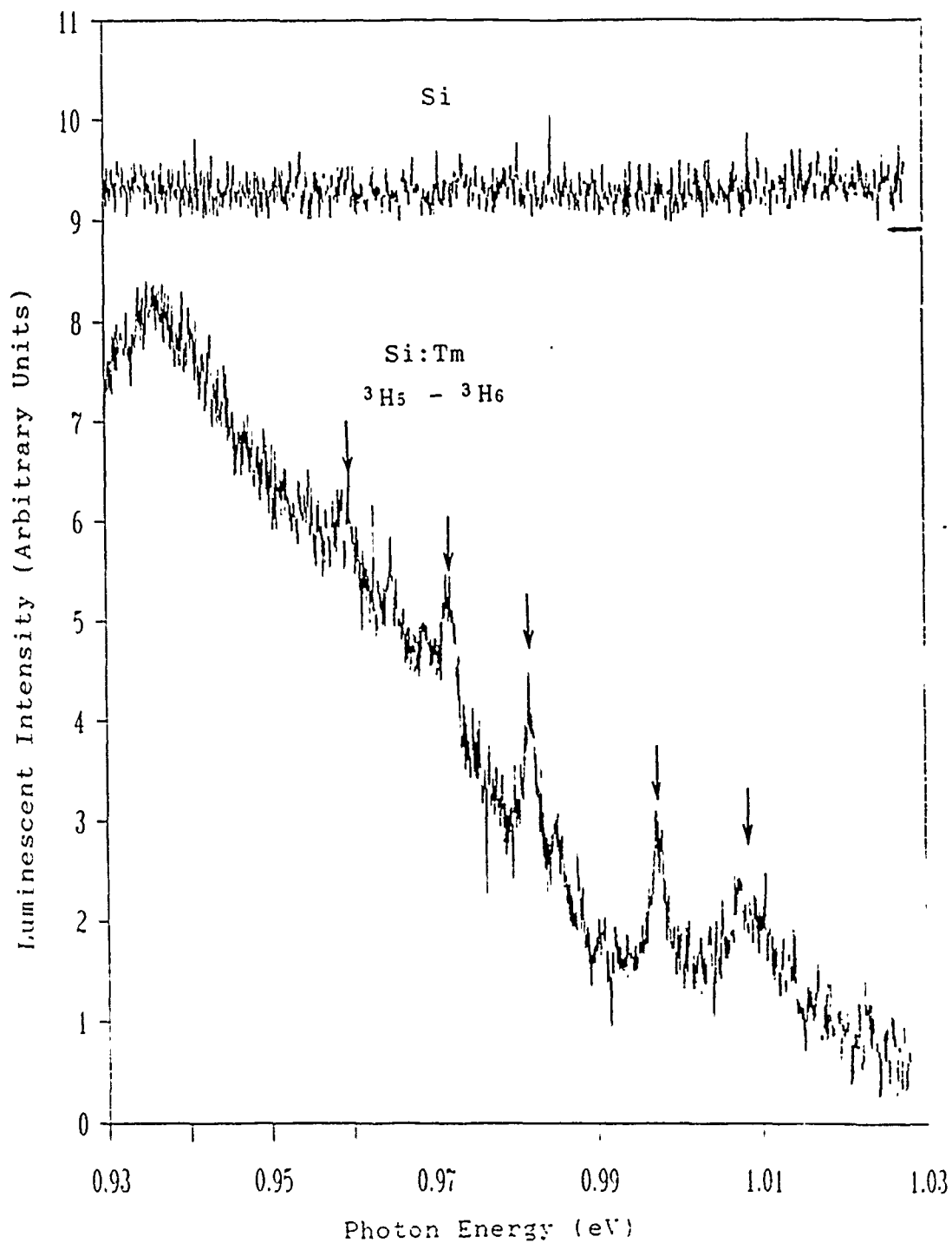
Figure 26. Comparison Spectra of Silicon Implanted with 390 keV Thulium (lower spectra) and Unimplanted Silicon (upper spectra). Both Samples were Annealed at 850°C for 15 min.

superimposed on a strong background signal. Also on Figure
26 is shown a spectra of the same region of an unimplanted
SI silicon (Wacker) sample annealed under the same
conditions. This sample shows no emissions in this region,
therefore the emissions seen in the first sample are due to
the Tm^{3+}. None of the peaks observed are at the same
energetic locations as in GaAs. This result testifies to
the fact that Tm^{3+} encounters a different crystal field in
silicon as compared to GaAs.

Figure 27 shows a comparison of the near-edge
emissions of the implanted and unimplanted samples. It is
clear that near-edge emissions are unchanged except in
intensity. The unimplanted sample showed much stronger
emissions. This result could point to energy transfer from
the near-edge emissions to the RE; however, reduction of the
near-edge emission intensity could have also resulted from
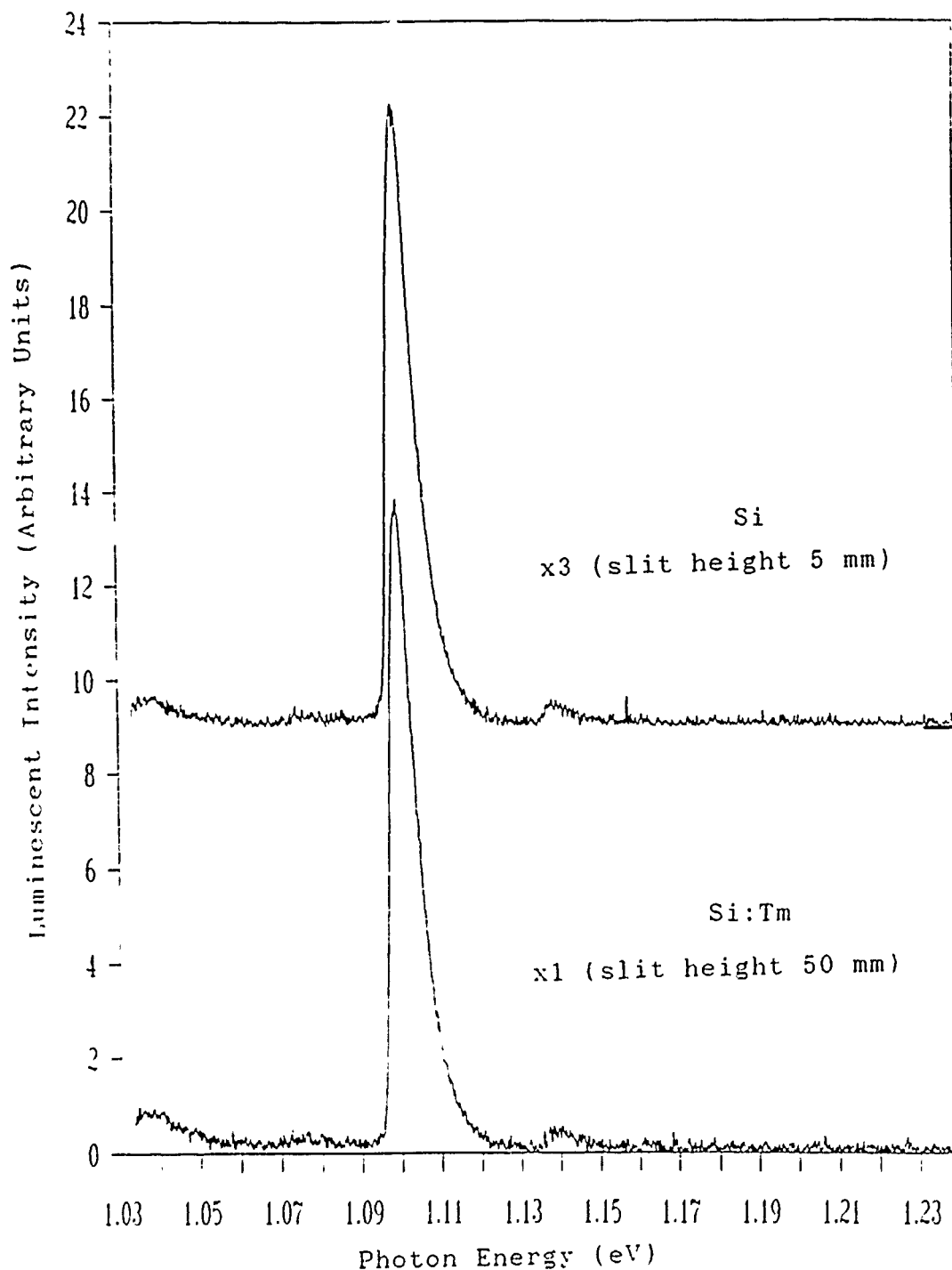implantation damage.

Figure 27. Comparison Spectra in the Near-Edge Region of Silicon Implanted with 390 keV Thulium (lower spectra) and Unimplanted Silicon (upper spectra). Both Samples were Annealed at 850°C for 15 min.

V. Conclusions and Recommendations for Future Study

Holmium implanted into Si, InP, and GaAs did not show any 4f emissions. SIMS studies on InP:Ho concluded that holmium was, in fact, implanted; however, it did not become optically active in these samples.

Further photoluminescence studies should be done with different excitation sources to see if the particular excitation frequency chosen (647.1 nm) did not allow for holmium 4f excitation. Also, electrical measurements could be performed on these samples to determine whether holmium doping in some way changes the electrical behavior of the semiconductor. Finally, other methods of placing holmium within the substrate, such as thermal diffusion or molecular beam epitaxial growth, could be tested. Perhaps another growth method will provide for a detectable holmium 4f signal.

From the thulium studies, several conclusions can be drawn. First, thulium implanted into AlGaAs gives a strong luminescence signal in the .93 to 1.03 eV (1.2 to 1.35 μm) region. Sharp lines are visible which persist to temperatures over 200 K. An anneal temperature over 700°C for 15 minutes is necessary to produce the most intense emissions. At 600°C anneal temperatures, a different type of Tm^{3+} center is observed. The trend of luminescence with anneal temperature implies that the thulium ions move

69

within the lattice as the anneal temperature increases to 700°C.

Power dependence studies of AlGaAs:Tm and GaAs:Tm show a sublinear dependence of excitation power with luminescent intensity. This result leads to the conclusion that at high excitation power Auger (non-radiative) processes compete with radiative decay mechanisms.

Further study of AlGaAs:Tm is needed to better understand the origin of the individual peaks observed in the $^3H_5$ to $^3H_6$ transition. Do they all arise from transitions from the lowest level of the $^3H_5$ manifold to the crystal field split $^3H_6$ manifold, or do some transitions arise from higher states within the $^3H_5$ manifold? Photoluminescent excitation spectroscopy needs to be performed to work out the energy level diagram of the crystal field levels. Also, the samples could be subjected to a magnetic field to Zeeman-split the levels and this might help to determine the crystal field splitting and absolute energy level positions.

Time decay measurements should also be performed on each line in the .93 to 1.03 eV (1.2 to 1.35 μm) region to discover if they are all due to one type of Tm^{3+} center. Time decay results would also help in determining the excitation mechanism of the thulium 4f shell.

More AlGaAs:Tm samples should be implanted to determine ideal anneal conditions and ideal aluminum

content. With the limited number of samples available at this time, no such studies could be performed.

Electrical measurements might be performed on the n- and p- type GaAs:Tm samples to resolve how thulium implantation may have affected these samples. Such a study might also help determine why these samples showed no thulium 4f emissions.

Finally, since only one Si:Tm sample was found to show the Tm^{3+} emissions, more undoped silicon should be implanted to further study these emissions.

Appendix

The Hamiltonian which describes a RE ion in a weak crystal field is given by (Pappalardo, 1978:187):

$$H = H_0 + H_{ee} + H_{so} + H_{cf}. \tag{A1}$$

The first ter   ·on over all n electrons.

$$H_0 = - \sum_{i=1}^{n} (\quad - Ze^2/r_i) \tag{A2}$$

where p_i is the momentum of the ith electron, m is the electronic mass, r_i is the distance from the ith electron to the nucleus, Z is the atomic number, and e is the electronic charge (Weissbluth, 1978:385). Within H_0 are the familiar terms of kinetic motion of the electrons and the coulomb attraction between the electrons and the nucleus (assuming the stationary nucleus model). The second term, H_{ee}, arises from electron-electron coulombic repulsion:

$$H_{ee} = \sum_{i<j} e^2/r_{ij} \tag{A3}$$

where r_{ij} is the distance between the electron labeled i and the electron labeled j. The summation only extends

72

over i<j for each value of j to insure that pairs of electrons are only counted once. The third term, H_{so}, is the spin-orbit interaction term. This term splits energy levels based on total angular momentum, L (which is a summation of the angular momenta of the individual electrons, l_i) and total spin, S (which is a summation of the spin angular momenta of the individual electrons, s_i).

$$H_{so} = \sum_i \delta_i(r_i)\ l_i \cdot s_i \qquad (A4)$$

The proportionality factor, δ_i, is given by:

$$\delta_i(r_i) = \frac{Ze^2 \hbar^2}{2m^2 c^2 r_i^3} \qquad (A5)$$

where $\hbar$ is Planck's constant divided by 2π, and c is the speed of light (Weissbluth, 1978:383). The fourth and final term, H_{cf}, is the crystal field splitting. This term's magnitude and symmetry depend entirely on the site in which the RE ion finds itself.

Bibliography

Adachi, S. "GaAs, AlAs, and $Al_xGa_{1-x}As$: Material Parameters for Use in Research and Device Applications," _Journal of Applied Physics, 58_: R1-R29 (1985).

Ashcroft, N. W. and Mermin, N. D. _Solid State Physics_. Philadelphia: Saunders College, 1976.

Benyattou, T. et al. "Radiative and Non-Radiative Recombinations at Er Centers in GaAlAs," _Impurities, Defects, and Diffusion in Semiconductors: Bulk and Layered Structures_, edited by D. J. Wolford et al. 69-74, 1990.

Blaauw, C. et al. "Metalorganic Chemical-Vapour-Deposition Growth and Charcterization of GaAs," _Canadian Journal of Physics, 63_: 664-669 (1985).

Blakemore, J. S. "Semiconducting and Other Major Properties of Gallium Arsenide," _Journal of Applied Physics, 53_: R123-R181 (Oct 1982).

Dean, P. J. "Photoluminescence as a Diagnostic of Semiconductors," _Progress in Crystal Growth Characterization, 5_: 89-174 (1982).

Dean, P. J. et al. "New Radiative Recombination Processes Involving Neutral Donors and Acceptors in Silicon and Germanium," _Physical Review, 161_: 711-729 (15 Sep 1967).

Dekeyser, W. C. "Crystal Structure," _Solid State Physics Source Book_ edited by Sybil Parker. New York: McGraw-Hill, 1988.

Di Bartolo, B. _Optical Interactions in Solids_. New York Wiley and Sons, 1968.

Eaves, L. et al. "An Investigation of the Deep Level Photoluminescence Spectra of InP(Mn), InP(Fe), and of Undoped InP," _Journal of Applied Physics, 53_: 4955-4963 (July 1982).

Ennen, H. and Schneider, J. "Luminescence of Rare Earth Ions in III-V Semiconductors," _Thirteenth International Conference on Defects in Semiconductors_ edited by L. Kimerling and J. Parsey, Jr. 115-127 New York: Conference Proceedings, 1984.

Imbusch, G. F. and Kopelman, R. "Optical Spectroscopy of Electronic Centers in Solids," Topics in Applied Physics, Vol. 49: Laser Spectroscopy of Solids (Second Edition) edited by W. M. Yen and P. M. Selzer. Berlin: Springer-Verlag, 1986.

Kabler, M. N. "Exciton," Solid State Physics Source Book edited by Sybil Parker. New York: McGraw-Hill, 1988.

Kasatkin, V. A. and Savel'ev, V. P. "Excitation of Ytterbium Luminescence in Gallium and Indium Phosphides," Soviet Physics: Semiconductors, 18: 1022-1023 (Sep 1984).

Kasatkin, V. A. et al. "Kinetics of the Electroluminescence of Ytterbium Ions in Indium Phosphide," Soviet Physics: Semiconductors, 19: 221-222 (Feb 1985).

Korber, W. and Hangleiter, A. "Excitation and Decay Mechanisms of the Intra-4f Luminescence of Yb^{3+} in Epitaxial InP:Yb Layers," Applied Physics Letters, 52: 114-116 (11 Jan 1988).

Mooser, E. "Bonds and Bands in Semiconductors," Crystalline Semiconducting Materials and Devices edited by P. Butcher et al. New York: Plenum, 1986.

Oberstar, J. D. and Streetman, B. G. "Photoluminescence Studies of ^{4}He- and ^{9}Be-Implanted Semi-Insulating InP," Journal of Applied Physics, 53: 5154-5162 (July 1982).

Pankove, J. I. Optical Processes in Semiconductors. New York: Dover, 1971.

Pappalardo, R. G. "Spectroscopy and Luminescence of Lanthanides and Actinides," Luminescence of Inorganic Solids edited by B. DiBartolo. New York: Plenem, 1978.

Pomrenke, G. S. Luminescence of Lanthanides and Actinides Implanted into Binary III-V Semiconductors and AlGaAs. PhD dissertation. School of Engineering, Air Force Institute of Technology (AU), Wright-Patterson AFB OH, Dec 1989.

Pomrenke, G. S. et al. "Photoluminescence from Mg-Implanted, Epitaxial, and Semi-Insulating InP," Journal of Applied Physics, 52: 969-977 (Feb 1981).

Queisser, H. J. and Fuller, C. S. "Photoluminescence of Cu-Doped Gallium Arsenide," _Journal of Applied Physics, 37_: 4895-4899 (Dec 1966).

Solomon, J. S. et al. "SIMS and Photoluminescence Studies of Rare Earth Implants in InP," _Secondary Ion Mass Spectrometry (SIMS VII)_ edited by A. Benninghoven et al. 571-574 New York: Wiley, 1989.

Sze, S. M. _Physics of Semiconductor Devices_ (Second Edition). New York: Wiley, 1981.

Takahei, K. et al. "Photoluminescence Characterization of Rare-Earth (Er,Yb)-Doped InP Grown by Metalorganic Chemical Vapor Deposition," _Journal of Luminescence,_ _40&41_: 901-902 (1988).

Takahei, K. et al. "Intra-4f-Shell Luminescence Excitation and Quenching Mechanism of Yb in InP," _Journal of Applied Physics, 66_: 4941-4945 (15 Nov 1989).

Walter, U. "Treating Crystal Field Parameters in Lower than Cubic Symmetries," _Journal of Physics and Chemistry of Solids, 45_: 401-408 (1984).

Wang, Z. G. et al. "Acceptor Associates and Bound Excitons in GaAs:Cu," _Journal of Applied Physics, 58_: 230-239 (01 July 1985).

Weissbluth, M. _Atoms and Molecules_. New York: Academic Press, 1978.

REPORT DOCUMENTATION PAGE

Public reporting burden for this collection of information is estimated to average 1 hour per response, including the time for reviewing instructions, searching existing data sources, gathering and maintaining the data needed, and completing and reviewing the collection of information. Send comments regarding this burden estimate or any other aspect of this collection of information, including suggestions for reducing this burden, to Washington Headquarters Services, Directorate for information Operations and Reports, 1215 Jefferson Davis Highway, Suite 1204, Arlington, VA 22202-4302, and to the Office of Management and Budget, Paperwork Reduction Project (0704-0188), Washington, DC 20503

1. AGENCY USE ONLY (Leave blank)	2. REPORT DATE December 1990	3. REPORT TYPE AND DATES COVERED

4. TITLE AND SUBTITLE
LOW TEMPERATURE PHOTOLUMINESCENCE STUDY OF HOLMIUM AND THULIUM IMPLANTED INTO III-V SEMICONDUCTORS AND SILICON

5. FUNDING NUMBERS

6. AUTHOR(S)
Eric Silkowski, 1 Lt, USAF

7. PERFORMING ORGANIZATION NAME(S) AND ADDRESS(ES)
Air Force Institute of Technology, WPAFB, OH 45433-6583

8. PERFORMING ORGANIZATION REPORT NUMBER
AFIT/GEP/ENP/90D-7

9. SPONSORING/MONITORING AGENCY NAME(S) AND ADDRESS(ES)

10. SPONSORING/MONITORING AGENCY REPORT NUMBER

11. SUPPLEMENTARY NOTES

12a. DISTRIBUTION AVAILABILITY STATEMENT
Approved for public release; distribution unlimited.

12b. DISTRIBUTION CODE

13. ABSTRACT (Maximum 200 words)
Low temperature photoluminescence studies were performed on holmium implanted into InP, GaAs, and Si; and thulium implanted into AlGaAs, GaAs, and Si. Samples were annealed by the conventional furnace and rapid thermal techniques. None of the characteristic 4f emissions of holmium were found in the spectral region of .73 to 1.55 eV. AlGaAs:Tm showed strong thulium emissions in the .93 to 1.03 eV region. These emissions were studied and compared to those in GaAs:Tm. Low and high temperature annealed samples showed evidence of trivalent Tm centers. Temperature dependence studies showed that thulium 4f emissions were present above 200 K but quench by 240 K. Laser excitation power dependence studies showed that the luminescent intensity of the main thulium 4f line depends linearly on the square root of laser power. This result implies that non-radiative decay mechanisms compete with the excitation and subsequent radiative decay of the thulium 4f shell. Also observed for the first time were thulium 4f emissions in the .93 to 1.03 eV region in high purity silicon implanted with thulium.

14. SUBJECT TERMS
Photoluminescence, Rare Earths, Thulium, Holmium

15. NUMBER OF PAGES
86

16. PRICE CODE

17. SECURITY CLASSIFICATION OF REPORT	18. SECURITY CLASSIFICATION OF THIS PAGE	19. SECURITY CLASSIFICATION OF ABSTRACT	20. LIMITATION OF ABSTRACT
Unclassified	Unclassified	Unclassified	UL